DEPARTMENT OF CHEMISTRY

ALEXANDRE DESCALÇO GIL

BSc in Cellular and Molecular Biology

BLOOD BRAIN BARRIER (BBB) PERMEA-BILITY STUDIES OF NOVEL LIPID NANO-PARTICLES (LNPS) FOR THE DELIVERY OF PROMISING DRUGS IN ALZHEIMER DISEASE

MASTER IN BIOMATERIALS AND NANOMEDICINE

NOVA University Lisbon September, 2024





DEPARTMENT OF CHEMISTRY

BLOOD BRAIN BARRIER (BBB) PERMEA-BILITY STUDIES OF NOVEL LIPID NANO-PARTICLES (LNPS) FOR THE DELIVERY OF PROMISING DRUGS IN ALZHEIMER DISEASE

ALEXANDRE DESCALÇO GIL

BSc in Cellular and Molecular Biology

Adviser: Dr. José Rui Ribeiro da Cruz Pereira

Associate Researcher, Instituto de Investigação e Inovação em Saúde - Universidade do Porto

Co-advisers: Professor Dr. Pedro Viana Baptista

Full Professor, NOVA School of Science and Technology, NOVA University Lisbon

Examination Committee:

Chair: Professor Dr. Luís Alexandre Almeida Fernandes

Cobra Branco

Associate Professor, NOVA School of Science and Technology, NOVA

University Lisbon

Rapporteurs: Dr. Diana Isabel Lourenço Matias

Junior Researcher, Instituto de Medicina Molecular João Lobo Antunes -

Faculdade de Medicina - Universidade de Lisboa)

Adviser: Dr. José Rui Ribeiro da Cruz Pereira

Associate Researcher, Instituto de Investigação e Inovação em Saúde -

Universidade do Porto

BLOOD BRAIN BARRIER (BBB) PERMEA-BILITY STUDIES OF NOVEL LIPID NANOPARTICLES (LNPS) FOR THE DELIVERY OF PROMISING DRUGS IN ALZHEIMER DISEASE
Copyright © Alexandre Gil, NOVA School of Science and Technology, NOVA University Lisbon.
The NOVA School of Science and Technology and the NOVA University Lisbon have the right, perpetual and without geographical boundaries, to file and publish this dissertation through printed copies reproduced on paper or on digital form, or by any other means known or that may be invented, and to disseminate through scientific repositories and admit its copying and distribution for non-commercial, educational or research purposes, as long as credit is given to the author and editor.

v

ACKNOWLEDGMENTS

To achieve these results and to conquer my objectives a lot of work was done behind the scenes. For that, I would like to express my deepest gratitude to everyone involved in this journey.

Firstly, I would like to thank my supervisor, Dr. Rui Pereira, for all the time spent throughout this year accompanying me throughout the different challenges faced during this work, and for all the guidance in overcoming them. I would also like to thank my co-supervisor Professor Dr. Pedro Viana Baptista for all the help and guidance both for this work and for the previous years of teaching, and above all for introducing to me this wonderful and mysterious world of nanomedicine that fascinated me so much

I would also like to express my deepest gratitude to Dr. Helena Azevedo, head of the Molecular Biomaterials group for receiving me in her lab and allowing me to perform this research. Together, I would also like to thank all the lab personnel and colleagues who have worked with me throughout this year and have helped and taught me a lot for this work to be possible.

I would like to thank all the external collaborators of the lab, Dr. Stoyan Smoukov, head of the Active and Intelligent Materials Laboratory from the Queen Mary University of London, who kindly provided us with the nanoparticles for this work, and Dr. Isabel Cardoso from the Molecular Neurobiology Laboratory at i3S that also provided us with other materials used in this work.

Regarding funding for the development of this project, I would like to express my gratitude to Fundação para a Ciência e a Tecnologia and the generous support of the iDMT Consortium for Nanodroplet Technologies Ltd. with experimental facilities.

I would like to express my gratitude towards my family who, despite not understanding most of what I've been doing for the past year, still provided with their unconditional love and support to achieve my goals.

I would also like to thank all my friends, both those that I made along this journey as well as the ones that have been with me from the start, with whom I've shared a lot of laughs.

Finally, I would like to thank my amazing partner, who has been by my side for this incredible roller coaster of emotions, for lending me a shoulder when I needed the most, for cheering me up when I was at my lowest, and for always stealing me a smile, even in the direct of times.

ABSTRACT

Dementia is one of the most common events associated with brain aging, estimated to reach 139 million people in 2050, with Alzheimer's disease (AD) being its most prevalent form. The blood brain barrier (BBB) acts as a wall for blood circulating substances and blocking 98% of brain-targeted drugs. Solid lipid nanoparticles (SLNPs) have shown promising potential as therapy vehicles for neurological disorders. They are commonly composed of a solid lipidic core surrounded by a surfactant layer, providing an efficient biocompatible carrier to transport therapeutic agents through BBB. The aim of this work consists of characterizing a novel SLNP formulation, assessing their potential as delivery systems for AD therapy.

SLNPs, supplied by external collaborators, were incubated for different periods at room temperature and 37 °C, in ultrapure water and endothelial basal medium, mimicking *in vitro* conditions, and physico-chemically characterized. These presented high size stability (103.69 \pm 3.18 nm and 56.39 \pm 0.78, for batch#1 and #2 respectively) throughout the incubation periods in both solvents. A slight size increase was reported as consequence of cluster formation due to the increase in temperature, allowing for the lipidic particles to get closer together, with transmission electron microscopy confirming these results.

Cytotoxicity of SLNPs on human brain microvascular endothelial cells was assessed and cell uptake capacity by flow cytometry and confocal microscopy. These show signs of harmful behavior towards cells, indicating a possible problem with the formulation. A lack of internalization of lower, non-toxic, concentrations of SLNPs was also reported. The individual components were assessed, identifying Brij S20 as the root of the toxicity issue.

This work proposes the complete removal of this surfactant from the formulation, its decrease in concentration to 0.05% (w/v) of the final formulation or the development of a purification process of the system, drawing out the true potential of the SLNPs.

Keywords: Alzheimer's Disease, Blood Brain Barrier, Cytotoxicity, Precirol® ATO5, Solid Lipid Nanoparticles, Surfactants.

The research work described in this dissertation was carried out in accordance with the norms established in the ethics code of Universidade Nova de Lisboa. The work described and the material presented in this dissertation, with the exceptions clearly stated, constitute original work carried out by the author.

RESUMO

Demência é um dos eventos mais comuns associados com o envelhecimento, sendo estimado atingir cerca de 139 milhões de pessoas em 2050, sendo a doença de Alzheimer (AD) a sua manifestação mais comum. A barreira hematoencefálica (BBB) funciona como uma barreira para substâncias presentes no sangue, bloqueando 98% de fármacos para doenças neurológicas. Nanopartículas lipídicas sólidas (SLNPs) exibem potencial como terapias para estas doenças. São compostas por um núcleo lipídico sólido revestido por surfactantes, proporcionando um transportador eficiente e biocompatível para atravessar a BBB. O objetivo deste trabalho consiste na caracterização de uma nova formulação de SLNPs, averiguando o seu potencial como agentes de transporte para tratamento de AD.

SLNPs foram fornecidas por colaboradores externos e incubadas por diferentes períodos, a temperatura ambiente e 37 °C, em água ultrapura e meio endotelial basal, mimetizando condições *in vitro*, sendo posteriormente físico-quimicamente caracterizadas. Estas apresentam tamanho estável (103.69 ± 3.18 nm e 56.39 ± 0.78 , para os lotes #1 e #2 respetivamente) ao longo do tempo, e em ambos os solventes. Um pequeno aumento no tamanho foi reportado, uma consequência do aumento de temperatura, induzindo a proximidade entre partículas, tendo microscopia eletrónica de transmissão confirmando estes resultados.

A citotoxicidade das SLNPs foi verificada em células endoteliais da microvasculatura cerebral humana e a internalização foi estudada por citometria de fluxo e microscopia confocal. Estas apresentam comportamento nocivo para com as células, indicando possíveis problemas na formulação. A ausência de internalização destas partículas em concentrações mais baixas, não tóxicas, foi também reportada. Os componentes das SLNPs foram individualmente estudados, identificando Brij S20 como a causa de toxicidade.

Este trabalho recomenda a remoção completa deste surfactante da formulação, a diminuição da sua concentração para 0.05% (w/v) da formulação final ou o desenvolvimento de um processo de purificação do sistema, promovendo o verdadeiro potencial destas SLNPs

Palavras-Chave: Barreira hematoencefálica, Citotoxicidade, Doença de Alzheimer, Nanopartículas lipídicas sólidas, Precirol® ATO5, Surfactantes.

O trabalho de investigação descrito nesta dissertação foi realizado de acordo com as normas estabelecidas no código de ética da Universidade Nova de Lisboa. O trabalho descrito e o material apresentado nesta dissertação, com as exceções claramente indicadas, constituem trabalho original realizado pelo autor.

CONTENTS

1	INT	RODUCTION	1
	1.1	Alzheimer's Disease	1
	1.2	Blood Brain Barrier	5
	1.3	Nanoparticles to cross the BBB	11
2	MA	TERIALS AND METHODS	15
	2.1	Preparation of the nanoparticles	15
	2.2	Surfactant solutions preparation	15
	2.3	Characterization of the SLNPs	16
	2.3.1	Size and charge	16
	2.3.2	Transmission Electron Microscopy	16
	2.3.3	pH assessment	17
	2.3.4	SLNP fluorescence quantification	17
	2.4	Stability assessment of SLNPs	17
	2.5	Cell culture preparation	18
	2.5.1	MTT solution preparation	19
	2.5.2	SLNP cytotoxicity	19
	2.5.3	Optimal surfactant range	20
	2.6	Cell internalization assays	20
	2.6.1	Flow Cytometry - FACS	20
	2.6.2	Confocal microscopy	21
	2.7	Statistical analysis	21
3	RES	ULTS AND DISCUSSION	23
	3.1	Characterization of the SLNPs	23
	3.1.1	Size and charge	23
	3.1.2	Morphology	25
	3.1.3	pH	26
	3.1.4	Fluorescent intensity	27
	3.2	Stability of the SLNPs	29
	3.2.1	Effect of temperature in the stability	29
	3.2.2	Effect of the solvent in the stability	32

	3.3	Cytotoxicity assay	34
	3.3.1	SLNP cytotoxicity	34
	3.3.2	Cytotoxic agent identification	36
	3.3.3	Optimal surfactant range	37
	3.4	Cell internalization assays	38
4	Con	NCLUSIONS AND FUTURE PERSPECTIVES	4 1
A	APP	ENDIX	51
	A.1	DLS results of the surfactant samples	51
	A.2	DLS results of SLNPs incubated at 37 °C over time	51

LIST OF FIGURES

Figure 1.1. Schematic representation of the different events during AD.	3
Figure 1.2. Schematic representation of the Brain microvascular environment, its constituent	s and
transport routes across it	6
Figure 1.3. Schematic representation of the different in vitro BBB culture models.	10
Figure 1.4. Chemical structure of the different components of the SLNPs	
Figure 3.1. TEM Images of the SLNPs and surfactant solutions tested for characterization	26
Figure 3.2. Fluorescence intensity of increasing concentrations of FITC-labelled SLNPs (0.	0001
$0.0005,0.001,0.0025,0.005,0.010,0.025,0.050,0.500,50,500$ and $1000~\mu g/m L).$	28
Figure 3.3. Stability assessment of SLNPs (50 μg/mL) incubated at room temperature (~25 °C) and
37 °C in water throughout time periods of 0 h, 30 min, 1, 3, 6, 24, 48 and 72 h	31
Figure 3.4. Stability assessment of SLNPs (50 μg/mL) incubated in water and EBM-2 with 0.5%	FBS
throughout time periods of 0 h, 30 min, 1, 3, 6, 24, 48 and 72 h.	34
Figure 3.5. Cell Viability assessment of hCMEC/D3 and optical microscopy pictures taken after	6h of
incubation with different concentrations of SLNPs.	35
Figure 3.6. Cell viability assay of DAOY cell line incubated with 50 μg/mL of SLNPs	36
Figure 3.7. Cell viability of hCMEC/D3 incubated with 500 ng/mL (A) and 5 ng/mL (B) of SLNPs	s ovei
6, 24, 48 and 72h	
Figure 3.8. Cell viability of hCMEC/D3 cells incubated with 50 µg/mL of SLNPs and its respectively.	
components in the same concentrations.	37
Figure 3.9. Cell viability of hCMEC/D3 cells with different concentrations of individualized surface and combined.	
Figure 3.10. Confocal microscopy image of hCMEC/D3 cells untreated with SLNPs (A) and after	
of incubation with 500 ng/mL of SLNPs (B).	
Figure A.1. Raw DLS results of surfactant samples with their representative peaks highlighted becomes	-
arrows	51
rigure mass. Naw Deb results of bern s incubated in water at 37 °C 0ver unforth time periods	1

LIST OF TABLES

Table 1.1. FDA-Approved drugs for AD management and their action principles	4
Table 2.1. Samples analyzed for the characterization assays and their stock and working concent	rations.
	16
Table 2.2. Surfactant mix (Brij S20:Monoolein) and SLNP solution concentrations tes	sted for
cytotoxicity studies in hCMEC/D3 cell line	19
Table 3.1. SLNP and surfactant samples characterization, assessing Size, PdI, Zeta Potential, Sh	ape and
pH	24
Table 3.2. hCMEC/D3 SLNPs internalization analyzed by FACS.	39

ACRONYMS

 $egin{array}{ll} {\bf A}{\bf A} & {\bf A}{\bf mino~acid} \\ {\bf A}{f \beta} & {\bf A}{\bf myloid}{f -}{f \beta} \end{array}$

ABC ATP-Binding Cassette

ACh Acetylcholine

AD Alzheimer's DiseaseAJ Adherens Junction

APP Amyloid Precursor Protein

AQP-4 Aquaporin-4

ATP Adenosine Triphosphate

Aβ Amyloid Beta

BBB Blood Brain Barrier

BCRP Breast Cancer Resistance Proteins

BEC Brain Endothelial Cell

CMC Critical Micellar Concentration

CNS Central Nervous System

Cryo-Electron Microscopy

CSF Cerebrospinal Fluid

DAOY Medulloblastoma cell lineDLS Dynamic Light Scattering

DMEM Dulbecco's Modified Eagle Medium

DMSO Dimethyl Sulfoxide

EBM-2 Endothelial Basal Medium 2

F.U. Fluorescence Units

FACS Fluorescence Activated Cell Sorting

FBS Fetal Bovine Serum

FDA Food and Drug Administration

FITC Fluorescein Isothiocyanate isomer 1

GJ Gap Junction

GLUT1 Glucose Transporter Type 1

hCMEC/D3 Human Cerebral Microvascular Endothelial Cells

JAM Junctional Adhesion Molecule
LAT1 L-type Amino Acid Transporter

LRP1 Low-density lipoprotein receptor-related protein 1

MeHCl Memantine Hydrochloride

MRI Magnetic Resonance Imagi

MRI Magnetic Resonance Imaging
MRP Multidrug Resistance-associated Proteins

MTT 3-(4,5-Dimethyl-2-thiazolyl)-2,5-diphenyl-2H-tetrazolium Bromide

NFT Neurofibrillary Tangles

NLRP3 Nucleotide-binding oligomerization domain-like receptor pyrin domain-containing 3

NP Nanoparticle

NS Nervous System

NTS Neurotransmitter System
PBS Phosphate-Buffered Saline

PdI Polydispersity Index

Pen Strep Penicillin Streptomycin

PFA Paraformaldehyde
P-gp P-Glycoprotein

PLGA Poly(lactic-co-glycolic) Acid
PNS Peripheral Nervous System

PPARγ Peroxisome Proliferator-activated Receptor Gamma

RAGE Receptors for Advanced Glycation End Products

ROS Reactive Oxygen Species
SLNP Solid Lipid Nanoparticle

SPION Superparamagnetic Iron Oxide Nanoparticle

TEER Transendothelial Electrical Resistance
TEM Transmission Electron Microscopy

TfR Transferrin Receptor

TJ Tight Junction
TMPS Tramiprosate

VEGF Vascular Endothelial Growth Factor

ZO Zonulla occludens proteinsZO-1 Zonulla occludens protein 1

INTRODUCTION

1.1 Alzheimer's Disease

The central nervous system is a complex and important homeostasis and behavioral/functional regulatory system. It is responsible for the different sensations the human body can experience, a regulator of tissues and cells normal function, as well as the core structure for the processing and storage of information, producing the appropriate responses in the form of different stimuli [1]. Due to its role in maintaining and regulating the function of the different human body components, the nervous system (NS) spreads itself along the whole organism, being divided into two different parts, the peripheral nervous system (PNS) and the central nervous system (CNS). The PNS comprises neurons that extend from the spinal cord towards the different parts of the body, being responsible for receiving the different stimuli, transporting it into the brain and convey and exert the appropriate response in the organism[1]. On the other hand, the CNS consists of the spinal cord and the brain and is responsible for the storage and processing of information, interpreting it and generating the appropriate response. Within this system, the brain is considered the core element of the CNS, being responsible for the homeostasis and correct function of the different tissues in the human body [1,2].

The CNS can be divided into different components, each with their specific role in maintaining homeostasis and allowing for the survival and development of the organism [2]. Of these components, the brain can be divided into two hemispheres, the left, which focuses the most on the rational and logical behaviors and the right which is dominant in artistic behaviors. This process is known as brain lateralization and, together with the rest of the other components provide for the correct function of this system [1]. The outer layer of the brain is known as the cerebral cortex and is responsible for conducting high-level complex functions due to the high number of neurons present in this grey matter area. The cortex can further be divided into four zones, called lobes: frontal, parietal, occipital and temporal [1,3]. Each of these will be responsible for the execution of different functions and characteristics of the human behavior. For example, the temporal lobe takes part in processing different sensory inputs, allowing for the retention of information such as emotions and playing a very important role in memory [3].

Damages to the different parts of the NS can induce different types of responses and behavioral modifications, altering both the homeostasis as well as the correct function and survival of the individuals. When these damages or disease affect the cognitive function of the brain, a status referred to as dementia is acquired [4].

Dementia is the most common anomaly affecting old people, reaching around 55 million humans worldwide in 2019 and estimated to reach 139 million by 2050 [5–8]. Since dementia is a consequence of different factors that might influence the cognitive function of the brain and its homeostatic state, older people become more susceptible to develop these symptoms and present any sort of dementia-related diseases. The world health organization estimated in 2020 that around 1 billion people had over 60 years old, with this number doubling until 2050 and therefore increasing the risk of developing dementia throughout the years [6,9].

Different diseases might trigger this cognitive dysfunction, however, Alzheimer's disease (AD) is the most frequent form of dementia worldwide [5,7,9,10]. The most common symptom in AD is the

loss of memory. In this disease, changes in the normal brain function and in neuron's integrity will hinder the ability to create and retain memories. Thus, AD's dementia can be divided in three categories according to the severity of the symptoms: Mild, Moderate and Severe [6,7,9]. Mild Alzheimer's dementia is correlated with the earlier stages of this disease. Here, people will still be able to perform normal tasks independently, however, they might take more time doing so, even requiring some assistance in some activities. The moderate state is normally the longest and where the symptoms start to show the most. It's at this point that the patients will start having trouble in performing common tasks like bathing, experiencing more problems with memory and behavioral changes. When these symptoms aggravate even further, resulting in the constant need of care due to low cognitive abilities, the severe stage is reached. Here, most individuals become bed-bound due to the brain damage suffered, resulting in higher susceptibility for contracting other diseases, e.g. skin infections, and trigger generalized uncontrolled inflammatory responses leading to organ failure and eventually resulting in their death [6,7,9].

The most common symptom of AD is the uncontrolled loss of memory and the inability to create and store new memories. However, from a clinical perspective, this disorder is more complex, and the normal succession of events is still not fully understood. AD is characterized by a loss of cholinergic neurons, responsible for the storage of memories, excessive inflammation, abnormal accumulation of amyloid beta $(A\beta)$ plaques and hyperphosphorylation of tau proteins inside the neurons creating neuro-fibrillary tangles (NFTs) (Figure 1.1) [7,9,11,12]. Despite the full sequence of events not being defined, different theories have risen in order to better understand the progression and development of this disease and to better find a therapeutic target to treat this disease [5,7].

Throughout the years researchers have addressed the different symptoms of AD, aiming at understanding the underlying mechanism of this disease and its order of events. Following the most common symptom of AD, synaptic disfunction is considered to be one of the key factors regarding the appearance and development of this disorder [7,10,12,13]. At the neurons end feet, synaptic communication between these cells is dynamic and plastic, responding to the different modifications occurring at the dendrites, and is highly linked to learning and memory, with different studies addressing the cognitive decline and impairment of AD resulting as an effect of synapse loss/dysfunction, which leads to a decrease of neural signal transmission and to destruction of the neuronal network [7]. At the synaptic level different molecules are transferred from a neuron to the other, carrying with them the necessary stimulus to generate the adequate response to a specific sequence of events. These molecules are called neurotransmitters, and, out of these, Acetylcholine (ACh) has been reported to be intrinsically associated with AD. In 1986 Doucette et al. has reported a decrease in this neurotransmitter's level in AD patients [14]. ACh is synthesized in the presynaptic neurons and transported to the synaptic cleft where it is secreted and binds to receptors in the postsynaptic neuron, and is rapidly degraded. From this process, choline can be re-uptaken by the presynaptic neurons for ACh synthesis and to allow for this loop to go on. In AD there is a significant loss of both cholinergic neurons, responsible for ACh synthesis as well as this neurotransmitter, hence being considered another key factor in AD pathology [7,10]. In a healthy individual, Tau proteins are present inside the neurons and are responsible for assembling tubulin into microtubules, a very important cytoskeletal component, stabilizing them and allowing them to perform their correct function in maintaining the neuron's shape and function [7]. However, in specific cases and disorders such as AD, this Tau is hyperphosphorylated, leading to their aggregation and dissociation from the microtubules, inducing their destabilization [7,9–12,15]. With this, Tau NFTs will induce morphological changes in neurons, compromising their synaptic function, normal cellular functions, leading to neuroinflammation, oxidative stress and subsequent cell death [7]. However, from all these hypotheses, the amyloid cascade still seems to be the most supported theory as for the AD origin and progression [7,10,15]. In homeostatic conditions, amyloid precursor protein (APP) is catalyzed by an enzyme named α-secretase, generating soluble APPα fragments. However, in different diseases, such as Down Syndrome and AD, APP is catalyzed by β -secretase and then by γ -secretase [7,11,12]. This leads to the production of insoluble Amyloid-\(\beta \) (A\(\beta \)) fragments that rearrange themselves to form plaques in the patients brain. Different studies assessing mutations in the genes responsible for this change have addressed this issue as a responsible cause of not only the different subsequent events described by the other hypotheses, potentiating NFT formation, synaptic dysfunction, etc. but as a plausible cause for AD itself [7,15].

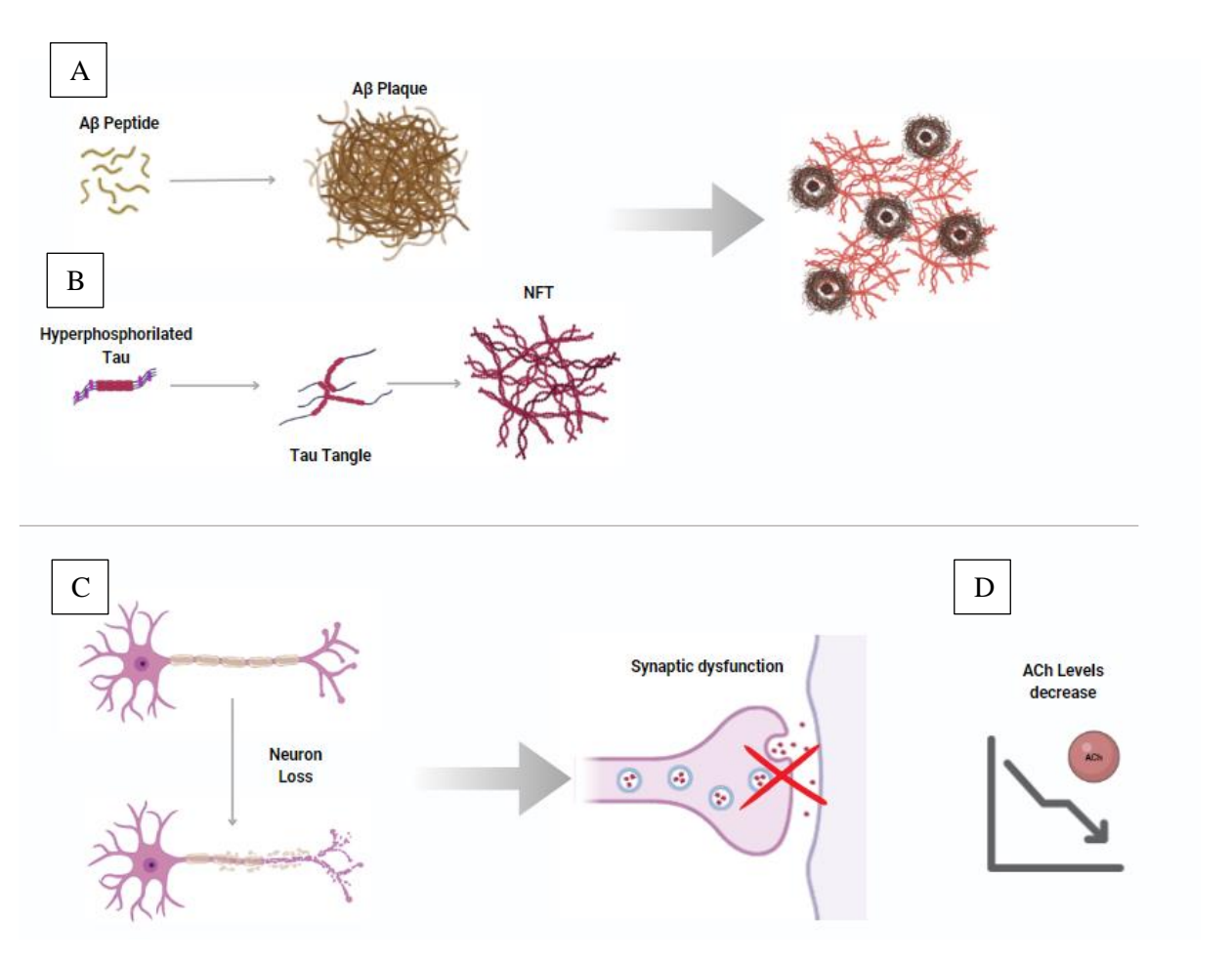


Figure 1.1. Schematic representation of the different events during AD.

The different events associated with AD pathology involve the production of $A\beta$ peptide due to issues in APP metabolic pathways, resulting in these insoluble fragments that rearrange in plaques and accumulate in the brain (**A**); the hyperphosphorylation of Tau proteins creating NFTs that influence the morphology of neurons, their correct function and leading to their death (**B**); the loss of cholinergic neurons, resulting in synaptic dysfunction (**C**); decrease of the levels of different neurotransmitters, specially Ach (**D**). Image created with BioRender.

Due to this complexity of AD, finding a treatment or cure is a very important and difficult task to achieve, having to combine different sorts of approaches involved in this disorder [7]. However, different attempts at such feat have been made throughout the years, with a few drugs already in the market and other different therapeutic approaches still in clinical trials and under development to respond to some unmet needs. Nowadays there are seven drugs that have been approved by the U.S. food and drug administration (FDA) for managing AD (Table 1.1) [9]. Despite none of these approaches being cures for the disease, they aim to improving its symptoms and promote treatment. The approved therapeutic approaches, as well as those under trial, can be categorized based on their objectives: (1) improving the symptoms of the disease or (2) treating the disease by targeting its underlying causes, aiming at the full recovery of the patient.

Most therapies that aim to improve the symptoms of the disease, both accepted and in trial are referred to as neurotransmitter system (NTS) associated, as they aim at managing the number of neurotransmitters available to compensate synaptic functions and improve the cognitive function [9,10,13]. This can be done by increasing its amount as 4 of the FDA approved drugs do, or by lowering the excess of neurotransmitters as memantine does, which lowers the levels of glutamate that overstimulates neuronal cells damaging them. These are the most common therapeutic approaches in AD, as they do not

aim at decreasing the biological associated hallmarks of the disease, allowing for other more desirable tailoring of the system [9,10]. Serving only as a "supplement" delivering small molecules that are able to cross the walls of the gut tract, thus allowing for the favorable oral administration over other routes, these therapeutics mostly aim for the delivery of agents that will trigger the increase of ACh levels at the target site, either by delivering acetylcholinesterase inhibitors, slowing the degradation of ACh delivering nicotinic agonists of ACh that act in the same way and induce the same biologic response, etc [10].

On the other hand, treatment-associated therapies affect the biology of this disease, targeting the possible origin of AD, slowing and, hopefully, stopping and reverting the progression of the disease [8–10,13]. Of these approaches, 2 therapeutic formulations have already been approved by the FDA [8,9]. Both of them are considered anti-aggregation therapies in the sense that they aim at removing A β plaques from the brain parenchyma. Other therapeutic agents of this type are now on clinical trials and have gain more reputation, being more common than NTS therapies. These not only seek to remove A β plaques but also NFTs, adding to their objectives the full inhibition of production, accumulation and toxic effect of these AD related components. To achieve this, researchers either promote the clearance of already present plaques by marking them with antibodies or by stopping their production by the administration of β -secretase inhibitors [10,13]. Other AD related biological changes include oxidative stress, inflammatory responses, excitotoxicity and cell apoptosis, however, fewer studies are in clinical trials that target these biological responses as these are not extensively documented as the other ones, highlighting their potential usefulness as further research is conducted on them [10].

Table 1.1. FDA-Approved drugs for AD management and their action principles. This table highlights the target mechanism of the drugs and their mode of action.

Name	Targeted mechanism	Type of agent	Action
Donepezil	Neurotransmitter system	Acetylcholinesterase in- hibitor	Preserve ACh levels in the synaptic cleft
Rivastigmine	Neurotransmitter system	Acetylcholinesterase in- hibitor	Preserve ACh levels in the synaptic cleft
Galantamine	Neurotransmitter system	Acetylcholinesterase inhibitor	Preserve ACh levels in the synaptic cleft
Memantine	Anti-excitotoxicity	NMDA receptor antago- nist	Prevents excess gluta- mate from over stimu- lating neurons
Memantine + Donepezil	Neurotransmitter system and anti-excitotoxicity	Acetylcholinesterase inhibitor and NMDA receptor antagonist	Preserve ACh levels and prevents glutamate overstimulation of neurons
Aducanumab	Anti-aggregation	Monoclonal antibody anti-Aβ	Promotes Aβ plaques clearance from the brain
Lecanemab	Anti-aggregation	Monoclonal antibody anti-Aβ	Promotes Aβ plaques clearance from the brain

However, despite the vast portfolio of in trial and pipeline AD-related therapies, there is also a major set of issues that compromises their success. In general, CNS targeted therapies have a very low success rate. In 2021, out of the 49 drugs approved by the FDA, only 7 were directed CNS-related disorders [13]. Not only this, but most of the drugs, independently of their administration route, have to consider the pathway that the therapy will have in the body, the different metabolic processes they might be involved, immunologic responses as well as the barriers to be crossed, e.g. the blood brain barrier (BBB), separating the brain from the blood and protecting it from the various toxins and harmful agents present in the blood [10]. One way of avoiding these hindrances, is through the combination of the therapeutic agent with a delivery vehicle, protecting it from the agents that might destroy it and further promoting the barrier crossing of the treatment. However, most AD-related therapies do not make use

of these delivery systems, which could benefit their formulations and better improve their therapeutic approach, kicking up the approval rate of these medicines [10].

1.2 Blood Brain Barrier

The correct function and homeostasis of the human body is dependent on the absorption and distribution of the correct nutrients and components throughout all the organs and tissues. The way to ensure that these organs are supplied with the correct set of components and that they reach their designed destination is through blood circulation. The way blood vessels are organized allows for the existence of capillaries which control this traffic/exchange of nutrients and gases through the tissue and the blood [16].

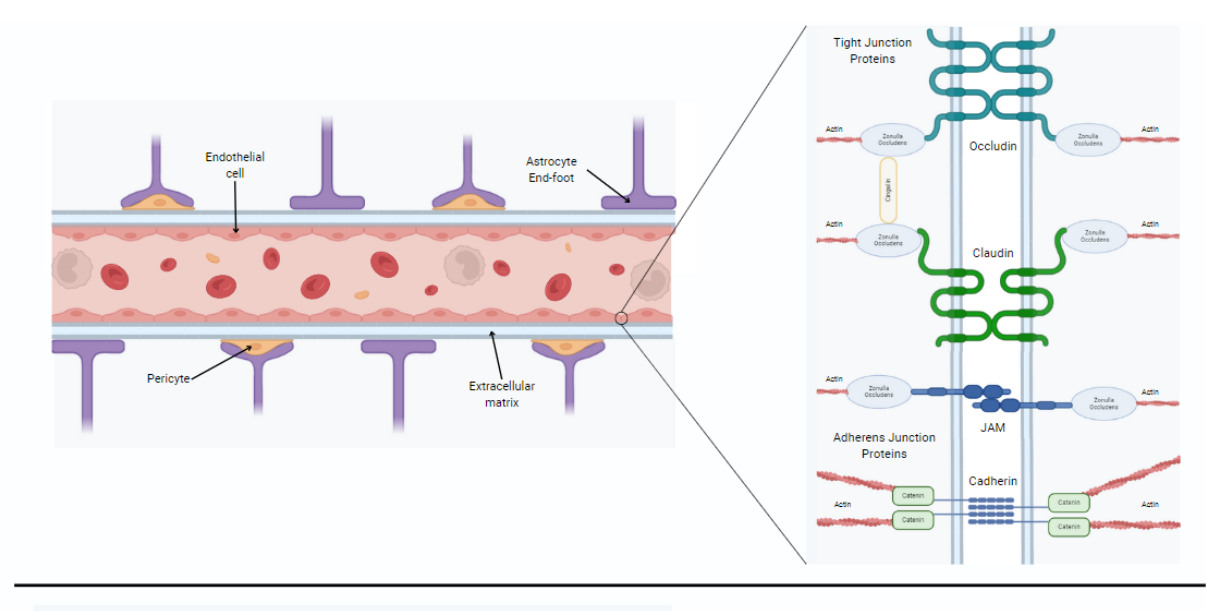
The capillary walls are constituted by a layer of endothelial cells followed by a basal membrane, creating a barrier that blocks the passage of undesired molecules towards the tissue in question. One example of these types of barriers is the BBB, whose main goal is to control the bi-directional transport of substances between the bloodstream and the brain parenchyma, allowing for the normal functions of the CNS [16–19].

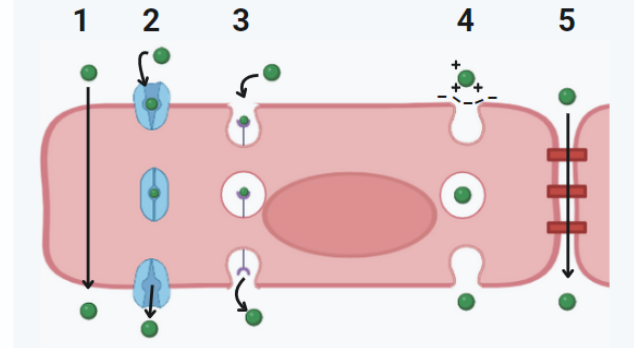
Aside from the endothelial monolayer and the basal membrane, the BBB is also constituted by vast cell types and other components such as astrocytes end-feet which are embedded in the basal membrane, neurons, pericytes, microglia and, together with the extracellular matrix and the previously described components, constitute the neurovascular unit responsible for the maintenance of the CNS homeostasis [19–21]. Despite this complex constitution, most research projects tend to focus on the study of the endothelial monolayer since this is the place where the main features that control the brain-blood traffic are located [21]. Being comprised of brain endothelial cells (BECs), this monolayer is characterized by the presence of Tight junctions (TJ), the arrest of pinocytic vesicles activity, the expression of efflux transporters and enzymes that metabolize bioactive substances. Each of these features play an important role in the maintenance of the integrity and function of the BBB and are what primarily defines their barrier capability [17,18,21].

BECs are anchored in the basal membrane and to each other through cellular junctions, more specifically, tight, adherens and gap junctions (TJ, AJ and GJ respectively). TJ and AJ are the ones that are mostly known about, with the GJ presenting unclear functional significance [17,21]. These structures are constituted by two domains, a transmembrane protein domain which is responsible for the gate-like appearance of the TJ, and a cytoplasmic plaque protein domain, which cluster in the same case, creating an interactive space between scaffolding and different signaling molecules, anchoring the transmembrane domain to the cellular cytoskeleton (Figure 1.2) [17,22–26].

TJs are specialized structures that regulate ions and other hydrophilic molecules' passage between cells, being the key component in blocking smaller molecules from transversing the BBB without being first recognized and transported across this barrier [21,25–27]. The transmembrane domain of the TJ is composed of various proteins, transmembrane ones with both intra and extracellular domains, as well as intracellular ones. Claudins are the core barrier forming proteins, whose extracellular loops determines the diffusion of molecules with a certain size due to the paracellular charge selectivity, thus resulting in higher Transendothelial Electrical Resistance (TEER) values, a measurement of the resistance towards the transport of molecules across the BBB [17,18,23]. Occludins, other proteins that are present in TJs, play a key role in the their assembly, being responsible for their gate resembling structure [17,24,25]. Together with claudins, these proteins are responsive to phosphorylation, changing their conformation and affecting their interaction with the intracellular proteins that are responsible for the cytoskeleton anchoring of the TJs [21,24,25]. Junctional adhesion molecules (JAM)-A, B and C are the last group of transmembrane proteins that are present in the BBB. They belong to the immunoglobulin superfamily and their interaction with each other forms dimmers which are present on the TJ structure. It is also believed that these proteins play an important role in the placement of zonulla occludens protein 1 (ZO-1) and occludin in the TJ structure [17,22,24,25,28]. Zonulla occludens proteins (ZO) on the other hand constitute the main intracellular domain of the TJ, providing for the cytoskeleton anchoring of the transmembrane proteins, as well as the distribution of the different protein components of the TJs. These ZOs are also bound to each other via cingulin proteins which bind with actin, regulating the localization of the different structural components of the cell [17,21,24,25].

AJ on the other hand are responsible for the interconnection between cells and their spatial placement towards each other, mediating their adhesion to each other [25]. AJs, similarly to TJs, are constituted by a set of transmembrane and intracellular proteins that form these structures. Cadherins constitute the main transmembrane proteins in AJs [17,21,24,25]. Their activity as signal mediators plays a key role in managing the cytoskeleton organization by activating phosphoinositide 3-kinase, forming complexes with vascular endothelial growth factor (VEGF) receptors 2 [17]. The C-terminus of cadherins directly binds to the intracellular proteins catenin, mainly α -catenin through a β -catenin linker, which binds to the actin network of the cytoskeleton of the cells. Therefore, cadherin plays an important role in maintaining the integrity of the endothelial cell layer present in the BBB while managing the placement and spatial configuration of new blood vessels [17,22,24].





- 1 Passive Diffusion
- 2 Carrier-mediated
- 3 Receptor-mediated
- **4** Adsorptive-mediated
- 5 Paracellular

Figure 1.2. Schematic representation of the Brain microvascular environment, its constituents and transport routes across it.

The complex brain microvascular environment is composed of different structures and cell types, including pericytes and astrocytes, separated from the BECs by the extracellular matrix basement membrane. Between endothelial cells there are present both tight and adherens junctions, which block the paracellular transport of the majority of substances to the brain. This results in the high selectivity to what molecules cross this barrier, and through their respective pathways. Image created with BioRender.

Another Interesting feature of the BBB is the expression and presence of different efflux transporters such as Adenosine Triphosphate (ATP)-binding cassette transporters (ABC Transporters). These pumps main goal is to release back into the bloodstream, through ATP hydrolysis, both endogenous and exogenous substances present in the brain parenchyma, conferring to the CNS drug resistance properties [21]. The most common transporter in these systems is the P-glycoprotein (P-gp) which, together with multidrug resistance-associated proteins (MRPs) and breast cancer resistance proteins (BCRP), provides

for a wide range of substrates to which it presents affinity, therefore protecting the CNS against different types of molecules, both endo and xenobiotics [17,21].

In the BBB environment there is also a high enzymatic activity, associated with the high expression of intra and extracellular drug metabolizing agents. These will allow for the production of an enzymatic barrier that, on one hand, can destroy deleterious agents that can cross the cell membrane to the interior of the endothelial cells, associated with a high metabolic activity inside these cells, but also as a result of the degradation of possible lipophilic xenobiotics that might present toxic behavior towards the brain into polar metabolites, hindering their chance to further cross the BBB [27,29,30].

During the assembly and formation of the BBB in the stages of embryonic development, the association of pericytes to the endothelial cells tends to interact with genes that are directly associated with the formation of pinocytic vesicles [18,25,26]. This results in a limited ability of the endothelial cells to transport different molecules through this route, however, depending on the characteristics and type of molecule, this type of transport is still present.

Although the transport of molecules through the BBB is highly controlled, it is not fully inhibited since the brain has a great need for different nutrients and energy. There are four different types of transport routes that, in normal conditions, a molecule might take when crossing the BBB: passive diffusion, adsorptive transcytosis, carrier-mediated and receptor-mediated transport [24,25,27].

Due to the different characteristics of the BBB just mentioned, very few molecules can passively diffuse through these membranes. Due to the lipidic nature of these membranes, the ability of a molecule to cross is highly dependent on the volume, weight and surface area and properties. Small lipid molecules with a molecular weight lower than 400 Da are the prime example of this kind of molecules [24,25,27]. Since the ability of a substance to cross a membrane decreases with the number of hydrogen bonds it forms, the higher the lipid solubility, the higher the possibility of a molecule to cross the BBB.

When a molecule presents itself with a positive charge, as a result of interactions between itself and proteins on the bloodstream, it will induce the invagination of the endothelial cells' membrane, creating an endosome vesicle, directly trafficking the molecule through the BBB, back to the bloodstream or into lysosomes for the destruction of the molecule [27,31].

Despite these mechanisms of transport seeming viable, the ones that are commonly used to transport the different nutrients to the brain consist of mediated transport systems, either by a specific carrier or receptor. In these two types of transport, carrier and receptor-mediated, the different molecules will be transported through the BBB differently [20,25,27].

In carrier-mediated transport, the passage of substances is performed with the assistance of a specific carrier that will transport it firstly into the endothelial cells and secondly from the cell into the basolateral side of the BBB. This transport works bi-directionally, being coordinated with the different efflux pumps already described, and normally used for hydrophilic molecules that both the brain and the endothelial cells might profit from uptaking [25,27]. One example of this transport system is the case of glucose which is imported with the help of the glucose transporters type 1 (GLUT1), which are present with high abundance in the endothelial cells, however, since this type of transport is dependent on the transporters, it is possible to reach a saturation period [17,20,25,27,32].

Receptor-mediated transport across the BBB, although similar to the carrier-mediated when considering the need of an intermediate molecule with which the substance will have to interact for the crossing, isn't directly transported into the endothelial cells and then to the basolateral side of the BBB. In this case, the molecule will interact with peptide receptors on the surface of the endothelial cells, and induce the invagination and endosomal vesicle formation, similar to adsorptive transcytosis, transporting the molecules into the brain, back to the bloodstream or simply uptaken to be used by the endothelial cells [20,24,25].

Despite its high selectivity towards the different molecules that are allowed to cross into the brain, BBB paracellular transport becomes a possibility when this barrier starts to lose its integrity [23,33].

The process of compromise or, as referred in the literature "BBB breakdown" consists of a natural phenomenon that occurs and evolves with the age of the individual. This is sometimes referred to as "healthy aging", in which natural cell aging damage accumulates and leads to different sorts of impacts in the BBB integrity such as oxidative stress, cell signaling impairment and dysregulation of inflammatory response, between others [25]. These physiological alterations usually induce cell degradation and/or shrinkage and the paracellular transport across the BBB becomes therefore a possibility since this results in the decreased expression and therefore presence of TJ proteins, as well as a compromise

of the normal transport routes [22,24,25]. On the other hand, so-called healthy aging can evolve into more severe stages and induce more deteriorating effects when a specific disorder or event takes place. The different conditions have their own molecular and physiological implications, each further enhancing the BBB breakdown with their specific pathways [25].

When BBB breakdown occurs, there are a few factors that remain common despite it being associated with healthy aging or induced by neurodegenerative disorders. One of those events is inflammation.

During inflammation cells from the microglia are activated leading to the recruitment of leukocytes that will cross the BBB, altering the paracellular and transcellular transport patterns as well as the TJ proteins expression, leading to the BBB breakdown. Another feature of the inflammation response is its interference with active efflux transporters, compromising the clearance of toxic substances inside the brain parenchyma, leading to further damage of the host CNS and BBB [22,24,25]. Other cell-cell interactions are also affected by an inflammatory response. Although not fully characterized yet, it is believed that the interactions between endothelial cells and astrocytes and pericytes change when there is an inflammatory response [34,35].

Oxidative stress is another factor that normally occurs and is responsible for BBB breakdown. This results from the compromised balance between oxidant-antioxidant species, resulting in the abundance of reactive oxygen species (ROS). From a pool of different species and radicals, containing superoxide, hydrogen peroxide, etc., reports suggest nitric oxide to be the principal species, being the root of the BBB endothelial damage [36]. With the more ROS consumption, the more susceptible the brain and endothelial cells become towards these species, interfering with different cellular pathways and gene expression, inducing the upregulation of inflammatory mediators, as well as altering the correct function of other cellular components such as TJ proteins, cytoskeleton reorganization, etc. [22,25].

If a person suffers from some sort of event or disorder that affects the brain, these incidents aggravate, being accompanied by a few others that also contribute to the BBB breakdown. For example, if a patient has an ischemic stroke, different soluble factors such as cytokines, VEGF and nitric oxide are released, resulting in the intensification of the inflammatory response and oxidative stress just described [22,24,25]. On the other hand, when considering brain tumors, the BBB permeability is mainly associated with the poor development of capillary endothelial cells [24]. According to different reports, claudin-1 protein expression is lost in microvessels of glioblastoma, accompanied by a significant down-regulation of claudin-5 and occludins, proteins associated with the formation of TJs [37]. Accompanied by the same events as the ischemic stroke, VEGF and cytokines secreted by some tumors also play a role in the downregulation of these TJs proteins, increasing therefore the vascular permeability [38].

The pathological characteristics of AD also influence inflammatory responses, oxidative stress and even promote other BBB breakdown routes. In these cases, AB plaques seem to be the root of the issue, interfering with the expression, structure and function of the different cellular components. The astrocyte degeneration in AD is associated with the decreased expression of some bidirectional water transport systems such as aquaporin-4 (AQP-4). These channels play a key role in Aβ clearance through the glymphatic system, a system responsible for the clearance and elimination of metabolites from the CNS, which, if not done correctly, might induce overly intense inflammatory responses and, as some studies shown, intracerebral hemorrhage in mice [22]. Not only this, but the actual interaction between Aβ and both astrocytes and microglia might activate the nucleotide-binding oligomerization domainlike receptor pyrin domain-containing 3 (NLRP3), leading to the release of different inflammatory mediators and inflammation [22,39]. Other BBB breakdown events linked to the presence of Aß plaques involve the TJ expression and correct function, therefore leading to increased permeability of the brain capillaries. It has been reported that the interaction between these plaques and receptors for advanced glycation end products (RAGEs) tends to disrupt the TJs by a calcium-calcineurin signalling pathway, accompanied also by structural changes of ZO1 and other TJ proteins such as claudin-5 and occludin, having even their expression reduced by A β [22,40]. It is also important to consider the fact that these proteins are positively bound with the presence of synaptic markers, which are decreased in AD. Finally, the low expression of different AB clearance mechanisms also play an important role in the BBB breakdown and disease progression [22,28]. The increased expression of RAGE, accompanied by the low expression of P-gp and Low-density lipoprotein receptor-related protein 1 (LRP1), transporters involved in clearance mechanisms, as well as the compromised function and reduced expression of GLUT1 transporters also promote the uptake of Aß into the brain and decrease the efflux of said plaques to the blood [22,28,39]. The LRP1 participates in other important BBB maintenance processes such as the stimulation of peroxisome proliferator-activated receptor gamma (PPARγ), increasing TJ expression. This effect has been studied in mouse models, with knockouts of LRP1, showing compromised expression of TJ proteins and P-gp transporters, leading to BBB breakdown [22]. Tau proteins also play a role in the BBB breakdown. In their normal conformation, they act in the stabilization and assembly of microtubules. However, the different conformational changes and modifications in an AD scenario trigger glial cell, inducing an inflammatory response and the consequent BBB breakdown [39].

To fully understand the different characteristics of the BBB, comprehend its function and develop different therapies that target the brain, there is a need to create the closest *in vitro* model that mimics the best barrier [41,42]. There are various issues regarding the use of *in vivo* models to study this structure varying from ethical concerns associated with the use of animal models, to actual physiological differences between these models and the human itself [16,41,42]. To date, different studies have provided evidence of differences in both anatomy as well as physiology between the human brain and BBB and the ones from the different animal models, specifically, mice. These differences have been noticed when comparing, for example, protein expression in the different organisms. For example, the expression of different protein-based receptors and transporters can vary between species. P-gp expression in the human BBB (6.06 ± 1.69 fmol/mg total protein) has been shown to be significantly lower than in mice (14.1 ± 2.1 fmol/mg total protein), accompanied by a lower transporter function as well [42]. The TJ protein expression also varies from humans to mice. Claudin-1, a TJ protein present in the human BBB is not expressed in mice parenchymal and meningeal blood vessel endothelial cells [42,43].

To tackle these inter-spices issues, human BBB *in vitro* models have been developed throughout the years. These can be divided into 2 categories: monocultures and multi-model cultures, each comprising different types of endothelial cells, either being immortalized cell lines, primary or stem cell cultures [16,18,41,42]. The use of primary cultures to create the models is associated with several drawbacks, ranging from regulatory frameworks and guidelines to the actual process of obtaining and culturing the cells, rendering them inefficient to use in cell models. With this in mind, *in vitro* BBB models could use stem cells, which allow for very promising barrier characteristics whilst meeting the requirements for large scale production, however, they are accompanied by a very complex differentiation process, rendering them inadequate [41,42]. Immortalized cell lines tend to be the most used when performing these models. These consist of primary cultures that suffered a mutation, either spontaneously or by chemical or viral factors, allowing for them to proliferate and be cultured for longer periods of time than primary cultures, whilst expressing the desired *in vivo* characteristics to some extent [41].

The difference between mono and multi-model in vitro cultures remains with the number of different cell types used in the culture (Figure 1.3). If the model is comprised of a single cell line, for example, immortalized human cerebral microvascular endothelial cells (hCMEC/D3) which is the first and better characterized immortalized cell line in BBB models, then it is considered a monoculture model [16,41]. A monolayer of these cells is grown on top of a semipermeable membrane that would simulate the basal membrane, in a structure called transwell, allowing for the study of drug permeability and transport across BBB models creating an "apical" side in which the endothelial cells are seeded, resembling the vascular side, and a basal side to where the molecules would cross, bellow the membrane, thus simulating the brain environment [18,25,33,41,42]. It is the most simplistic form of BBB models, being easily prepared with mild low cost and easily maintained and for that reason the best and most common choice for high throughput screening and preliminary permeability studies. On the other hand, multi-model cultures seed different cell types into the model to better mimic the in vivo BBB. To do that, researchers can co or tri-culture the different cell types involved in the neurovascular unit in different configurations, allowing for different assessment of properties, by assessing contact between different cell types in an oriented manner for example, by culturing astrocyte cells on the basal side of the membrane of the transwell, whilst the endothelial layer is on the apical side [41,42]. Despite better mimicking the BBB environment than the monoculture models, these imply a demanding maintenance with a more costly tailoring and optimization protocol, being much harder to work with, thus making the monoculture models the go-to BBB in vitro models.

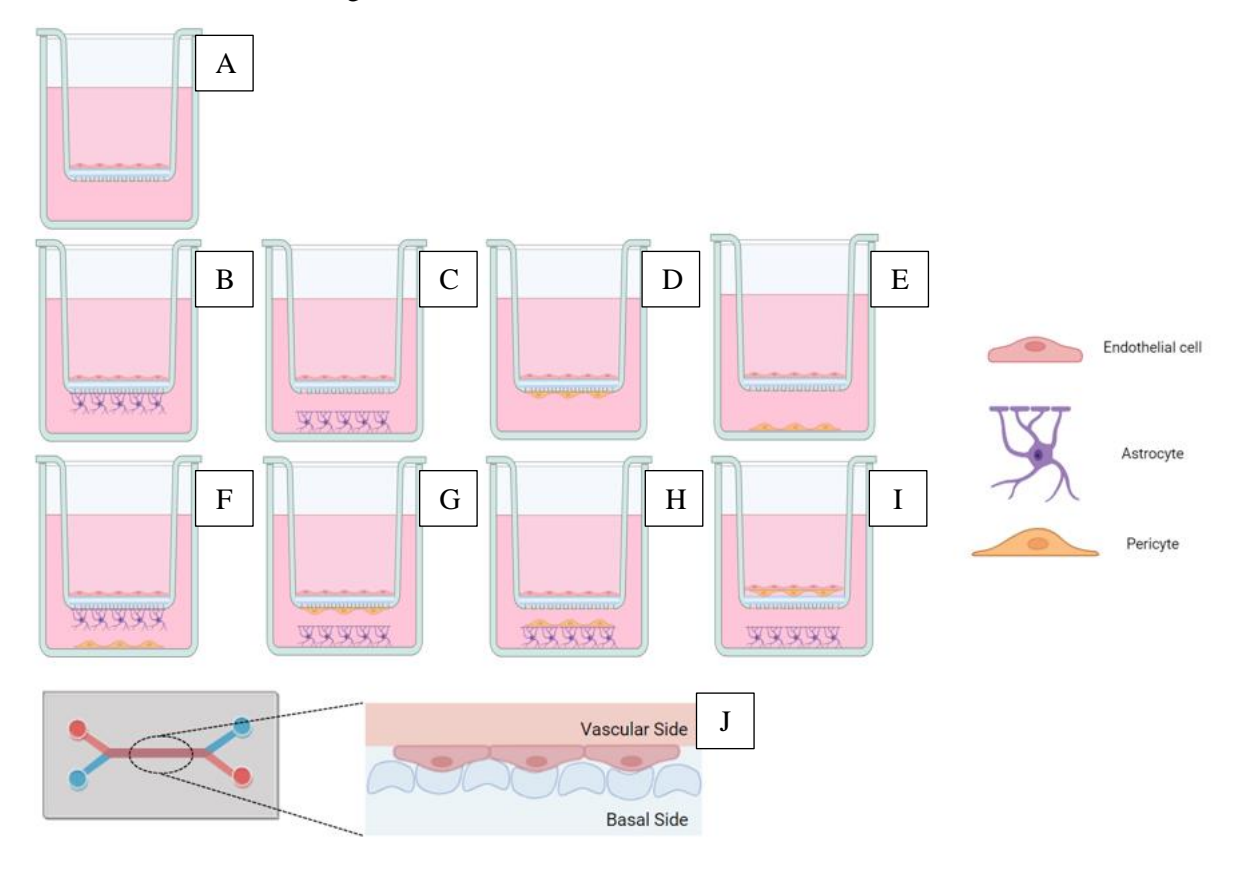


Figure 1.3. Schematic representation of the different in vitro BBB culture models.

(A) Monoculture containing only endothelial cells; (B) Co-culture of endothelial cells with astrocytes in contact; (C) Endothelial cells with astrocytes in co-culture without contact; (D) Endothelial cells with pericytes in co-culture with contact; (E) Co-culture of endothelial cells and pericytes without contact; (F) Tri-culture model involving endothelial cells, astrocytes and pericytes with astrocytes cultured on opposite side of filter; (G) Tri-culture model containing endothelial cells, astrocytes and pericytes with pericytes cultured on opposite side of filter; (H) Tri-culture model with endothelial cells, astrocytes and pericytes in a non-contact orientation; (I) Tri-culture model including endothelial cells, astrocytes with pericytes in close contact with the endothelial cells and astrocytes in a non-contact orientation; (J) Microfluidic ship model of the BBB where indentations of the chip allow for the separation of the vascular channel (red) from the basal channel (blue). Created with BioRender.

Different *in vitro* models of the BBB have been developed with the transwell model being the commonly used one. However, microfluidic chips have also been tailored to reproduce the BBB and its properties, successfully creating a useful model that mimics this barrier and allows for drug delivery studies [16]. Still, the complexity of the production and maintenance of these systems renders them ineffective when compared to simpler ones that allow for the same analysis with lower cost and maintenance procedures. Not only this, but the transwell models also allow for the modification of the cells seeded, creating different models of the same BBB in different conditions and disorders. This is also possible for AD, in which there is the BBB breakdown and disruption, as already described, which can be tailored by presenting the cells with actual A β peptides, enhancing the permeability and altering TJ proteins expression, by inducing peroxide oxidative stress, or by genetic manipulation of the cells involved in the model, creating a more fitting barrier behavior in cases of AD [22–24,33,39].

1.3 Nanoparticles to cross the BBB

When designing a drug formulation that targets the brain for the treatment of various diseases, one must take into consideration the already described characteristics of the BBB. Due to its high selectivity towards molecules and compounds, the scope of therapeutic agents that can be administered becomes narrow, limiting the possibilities available [31,44]. Due to the highly invasive nature of intracranial delivery, and the different surgical complications that might derive from it, the most widely accepted route of administration would be intravenously and, with this, another set of issues arise [45]. The fact that the body's immune system is prepared to recognize and deal with foreign materials makes it so that, even if able to cross the BBB, most drugs are not accumulated at the target tissue, being widely distributed through the body, rapidly cleared and demonstrating low stability in the plasma [44]. With this, the need of new strategies to improve the stability and effectiveness of these formulations must be investigated.

One way to overcome this problem would be to either avoid the BBB crossing or to enhance the therapy's ability to cross this barrier. Different strategies have emerged to bypass the BBB, aiming at a more efficient delivery of therapeutic agents to the brain. One example of these strategies is the intranasal administration of drugs to target other brain diseases such as seizures. These systems have been approved for the treatment of acute seizure clusters as fast and direct emergency intervention measurements, targeting the hippocampus through the lateral olfactory tract [20,21,26,31,44,46–49]. However, such a direct administration falls short when trying to tackle a more general disease such as AD, which could benefit from the extensive blood vessel networks in the brain, allowing for a more uniform distribution of the drug. In this context, the association of the therapeutic drug to a carrier, specifically, nanoparticles, surges as a promising approach.

Nanomaterials consist of agents whose dimensions are comprised between 1-100 nm. There are different types of these materials, ranging from nanoparticles (NPs), if all their directional axis are comprised in this scale range, nanorods if only two axes are within the nanoscale and sheet-like structures if only one of those axes is within 1-100 nm [50]. These materials can be used for different kinds of applications, either for sensors both in technological and the medical field, as contrast agents in the field of medical imaging, as theranostic agents and as both therapeutic agents and carriers of such [31,48,50–53]. NPs have provided a variety of approaches in all these application topics due to their versatility and differences between formulations. These systems can vary from each other depending on the material used to produce them, as well as their shape and size, which plays a very important role in the normal function of the NP. In this way, NPs can be divided into different categories, according to the parameter that distinguishes them, however, for this section of the work, the focus shines on inorganic, polymeric and lipid-based NPs [31,44,48,50].

The different composition of the NPs, alongside their morphology and size, play a very important role in regulating their abilities and properties, further influencing how they are going to act as therapeutic agents or carriers and in what field this activity will be observed [50]. For example, the size of the NPs is a very important factor when designing a carrier system since, usually the smaller the system, the easier it is to cross barriers and penetrate specific tissues. Not only that but it further influences its' clearing pathways, meaning that smaller particles are much easier to be excreted through urine than larger ones [54]. Morphology also plays an intertwined role with morphology in regulating the immune

system of the host, in a way that the shape of the particle can further influence the immune response [55]. The same happens with the size, the bigger the particle the easier it is for it to be detected. However, abnormal shapes might also be interesting to assess. For example, rod-shaped nanomaterials could be functionalized with different moieties, that allow for a better targeted therapy, between the tips and the body. This shape could also play a role in penetrating into tissues as it happens with carbon nanotubes [56]. Despite all these parameters that influence the properties of a nanomaterial, one must not overlook the importance of the composition of the nanomaterial.

The different materials that compose the nanomaterials will influence not only the stability and function of the system, but also impact the toxic response of the host, affecting the clearance and natural function of the human being, as well as providing a wide variety of options characteristics to be exploited [27,31,54,56]. For example, a wide variety of metallic NPs, when irradiated with a specific wavelength of light, generate heat due to a synchronized oscillation of the electrons on the surface of the NPs and therefore create a source of heat that could be used as an agent towards cancer therapy [48,57]. Superparamagnetic iron oxide NPs (SPIONs) behave on another way. By altering the magnetic field applied to an organism in which these agents were administered, SPIONs will behave as contrast agents, allowing for better resolution of magnetic resonance imaging (MRI) medical images [31,48,58]. Polymerbased NPs, such as poly(lactic-co-glycolic) acid (PLGA) promote a promising approach for drug delivery due to their biocompatibility and biodegradability, being already approved by the FDA and studied for crossing the BBB and brain uptake [31,44,48]. Lipid-based NPs also compete directly with the PLGA NPs, as they are composed of biocompatible materials with easy to synthesize, functionalize and load methodologies that are also biocompatible and degradable, also being implemented in the clinics, e. g.in recent events of COVID-19 with some of the RNA molecules in vaccination procedures being administered loaded into liposomes, a type of lipidic NP, as well as being extensively studied for crossing the BBB and drug delivery into the brain [19,21,31,44,47,48,59].

Despite their innate abilities and useful characteristics, NPs can still be further modified to allow for a better targeting of their therapeutic agents, mask their presence in the organism or even enhance their therapeutic efficacy [20,21,31,48]. To cross the BBB, different strategies have been adopted and studied with different types of NPs. The clearest example of such is the addition of targeting moieties for either the receptors or transporters on the surface of this barrier.

Functionalizing the surface of different NPs with glucose and other analogs and precursors to target GLUT1 is one of the most common strategies adopted in research when assessing transporter-mediated transcytosis. Due to the high amount of this transporter in the BBB, this approach deemed itself promising, even yielding very positive results, in improving the uptake of NPs across the BBB, and, even when loaded with doxorubicin to treat glioblastoma tumor, showing evidence of decreased tumor size [20,21,26,27,32,44]. Amino acid (AA) transporters have also been assessed to help the uptake of NPs across the BBB due to their ability to transport AA into the cells. One example of these transporters is the L-type amino acid transporter 1 (LAT1) which is highly expressed in brain tumor cells, as well as in the BBB, unlocking its' potential to help in the delivery of nano-systems to the brain [20,60]. By coating liposomes with glutamate, Li et al. [61] proved these transporters' efficacy in incorporating these AAs and their potential in brain tumor treatment. Additionally, these NPs also seemed to accumulate in the brain when assessed in intravenously injected mice, further highlighting the promising features of this transporter in aiding BBB passage.

Iron is a very important metal in the human organism, serving as a co-factor of various enzymes, thus, taking part in different metabolic pathways, one of which being the ATP synthesis [20]. Due to the high demand of energy by the brain, it is essential to have a secure route of supply of this metal to the brain parenchyma. That is accomplished by the Transferrin receptor (TfR), which is a transmembrane protein that induces endocytosis and secures the uptake of the brain by this molecule [20,31,45]. Another interesting property of this receptor is the fact that it is highly expressed in brain endothelial cells. Different lines of research took on the quest of functionalizing NPs with transferrin with the expectation of increasing the brain uptake of therapeutic agents [20,27,31,32]. *In vitro* studies of this functionalization's ability to cross the BBB have been successfully assessed in lipid and PLGA NPs, highlighting the promising features of this receptor into brain drug delivery [20,62]. This would be later confirmed by *in vivo* studies with zebra fish models by comparing the brain uptake of bare and transferrin-functionalized quantum dots, with sizes around 5 nm, and results supporting the higher uptake of the

functionalized ones, thus confirming the promising potential of this molecule as a targeting moiety [20.63].

Lipid-based NPs present promising approaches as drug delivery vehicles to the brain, with different properties that distinguish them from the other types of NPs. They provide a system with high drug delivery efficiency and loading capacity and variety, being able to transport hydrophobic and hydrophilic molecules, contrast agents, nucleic acids, etc. whilst also being biocompatible and with low toxicity. They are easy to produce and functionalize, either with stabilizing agents or targeting moieties for targeted therapy, and they provide a promising alternative to overcome the cost-effectiveness barrier that block other promising nanosystems [31,47,48,52,53]. The lipid composition of these NPs will highly influence their organization, properties, steric hindrance and, as a result, their application [31]. Different types of lipid-based NPs exist.

Liposomes are produced by the spontaneous organization of phospholipids in a bi-layer form, creating two compartments, a hydrophobic shell of phospholipids and a hydrophilic core. With this, liposomes can carry different types of therapeutic agents, hydrophobic in the bilayer and hydrophilic in the core, further enhancing their versatility in drug delivery. These are the most commonly studied type of lipidic NP when assessing, not only general drug/therapy delivery, but also brain drug delivery and BBB permeability studies [26,27,31,32,45,47,48,53].

The promising features of ionizable cationic lipids lead to the development of lipid NPs. These are characterized by the presence of lipids that present the ability to be positively charged at pH 4 whilst being electroneutral at physiological pH, providing for a safe solution for delivery platforms, with low toxicity and retarding the clearance from the reticuloendothelial system [19,47].

Differing from these, solid lipid NPs (SLNPs) do not present a hydrophilic core, rather they are composed of a solid lipidic one, surrounded by a layer of surfactants [31,47,48]. They are easier to produce when compared to liposomes with higher stability and efficiency of drug transport, being mainly derived from fatty acids rather than phospholipids [44,47,52,64]. Depending on the surfactants, the lipidic composition and charge of the SLNPs, these will behave differently and present different properties for targeted drug delivery and to cross the BBB [19,21,44,47,48,52]. These NPs present different advantages from their LNP counterparts, particularly in the fields of drug stability, availability and transport across the BBB. The tight lipidic matrix in the core of the SLNPs in a way limits the cargo that can be carried, but also provides for a higher stability for drugs loaded into it. This cargo capacity, although limited, still surpasses that of polymeric particles and some liposomes, therefore enhancing the availability aspect of these carriers [31,44,52]. Another aspect associated with this is the fact that, contrary to other lipid-based formulations, these SLNPs are produced in ways of being surrounded at least by a surfactant layer that will further enhance the retention time in the plasma and therefore compromising the opsonization of these carriers and their subsequent clearing, thus improving their retention time in the plasma. Associated to their accumulation in the blood vessels, these NPs will tend to be transported across the endothelial barriers and successfully release the drug cargo [21,44]. The different surface chemistry of the SLNPs plays an important role in the ability to cross the BBB. Some surfactants have shown properties capable of temporarily opening the TJs allowing for the crossing of these molecules, others allow for longer retention in the blood and therefore an easier transport across this barrier and, if further modified with stealth or targeting agents, even improve the accumulation at the targeted site and aiding in its transport through naturally implemented mechanisms [19,21,44]. Interestingly enough, a study comparing stealth and non-functionalized SLNPs demonstrated that, although the masked NPs are easier to cross the BBB, the pristine particles are also able to cross this barrier, highlighting the innate and interesting ability of these NPs to cross the BBB without the need for targeting moieties. However, these pathways are not well investigated, with further research being necessary. Nevertheless, functionalization further increases the availability and overall effectiveness of this system [48].

Different examples of SLNPs have been developed and modified to assess their usefulness in crossing the BBB. Most of these have been developed to deliver therapeutic agents to treat neurodegenerative disorders or brain tumors, however, an interesting study by Peira et al. tackled the possibility of loading SLNPs with SPIONs, successfully crossing the BBB, widening the field of application of these carriers as even for the targeted administration of MRI contrast agents [65]. Other studies focused on the development of SLNP therapy delivery systems for the treatment of various CNS disorders. A study from Shivananjegowda et al. evaluated the possibility of using SLNPs as a carrier of Tramiprosate

(TMPS) and memantine hydrochloride (MeHCl), a Aβ inhibitor and anti-glutaminergic drug respectively to manage AD. The authors were successful in achieving a system with a controlled steady release of their cargo whilst serving as a promising transport system across the BBB [64]. In another study by Vakilinezhad et al., aimed at developing SLNPs loaded with nicotinamide, demonstrated high potential in seizing AD progression. This combination showed promising results regarding the biodistribution and availability of this therapy to the brain, improving drug delivery and, consequently, the effectiveness of this system in improving cognitive response and preserving neuronal cells in AD pathology [66].

The aim of this work focuses on the characterization of a novel SLNPs formulation of Precirol (ATO 5) combined with two surfactants, Brij S20 and Monoolein (Figure 1.4) to assess their potential use for CNS drug delivery in AD. ATO 5 consists of a mixture containing palmitic and stearic acids, providing for a good biocompatibility and a looser structure that helps to entrap both hydrophobic and hydrophilic drugs, and has already been assessed for SLNP production [67]. Aside from this, Brij S20 was chosen as a surfactant as it allows for the stabilization of lipid-based systems and improves the bioavailability of the SLNPs, and Monoolein was used as a surfactant due to its amphiphilic properties, allowing for drug encapsulation and emulsification of the SLNP [68,69]. By combining these three components into a SLNP formulation, this work sought to characterize this system's properties and potential usefulness as a carrier of promising therapeutic agents for AD. Our studies consider the intravenous administration of this system, thus assessing the stability of these NPs in the different physiological conditions and their ability to permeate the BBB to successfully deliver the drug cargo.

Figure 1.4. Chemical structure of the different components of the SLNPs. **(A)** ATO 5; **(B)** Monoolein; **(C)** Brij S20.

MATERIALS AND METHODS

The main objective of the work presented in this dissertation consists of assessing the potential of a novel SLNP formulation as a potential drug delivery system to treat AD across the BBB. The formulation would enhance possible therapeutic effects of carried therapeutic agents by boosting its bioavailability to the damaged brain. Since this objective focuses on the usefulness of the novel formulation to be tested, no drugs and therapeutic agents are used. The methodologies employed in this work assess 5 principal topics: the preparation of this formulation (1) and its characterization (2), assessing the stability across different physiological conditions (3), verify possible SLNPs toxic effects (4) and assess uptake capacity on human endothelial cells (5).

2.1 Preparation of the nanoparticles

SLNPs used on the work were kindly produced and supplied by the Active and Intelligent Materials Laboratory from the Queen Mary University of London, providing with two batches of particles. NPs were constituted of 2% surfactants, of which 1.5% of Brij S20 and 0.5% of monoolein and by the main lipidic content, Precirol ATO 5 (Gattefossé, United Kingdom) with an amount of 0.5% in solution. Preparation was conducted by adapting the protocol by Lesov et. al., based on adjusting the temperature cycles towards the desired values [70]. Briefly, to create the lipid emulsion, ATO 5 was mixed with the aqueous surfactant mixture previously prepared and allowed to solubilize by increasing the temperature to 5-10 °C above its melting point, homogenized and then stored for 1 week before use at temperatures above the melting point of ATO 5. Afterwards, this solution was submitted to thermocycles of rapid cooling and slow heating through a flow reactor that allowed for the freezing of the lipid droplets as a consequence of the fast cooling of the system. Reaction cycles form empty spaces between lipidic clusters due to the polymorphic phase transitions associated with the slow heating process. This allows for the surfactant mixture to fill these cracks and induce the separation and fragmentation. The repeating of this procedure allowed for the formation of smaller lipidic particles, creating the SLNPs used in this study. Alongside with these SLNPs, the same collaborators also provided Fluorescein isothiocyanate isomer 1 (FITC)-labeled NPs (0.1% w/v), Batch#2, as well as the different components that form these SLNPs individually.

2.2 Surfactant solutions preparation

Apart from the provided SLNP solution, as controls, three stock solutions of surfactants were prepared. Brij S20 solution was prepared by weighting 22.5 mg and solubilizing them in 1.5 mL of ultrapure filtered MilliQ water. Sample was heated to 50 °C in a water bath (Emerson Electric Co., United States of America) and vortexed (J.P. SELECTA s.a., Spain) until completely solubilized, achieving a final concentration of 15 mg/mL. Monoolein stock solution was performed following a similar procedure. In brief, 7.5 mg were weighted and solubilized in ultrapure filtered MilliQ water, achieving a final concentration of 5 mg/mL. The physical mixture of surfactants was prepared by

weighting the same masses for each surfactant and adding them together. This combination was then solubilized in ultrapure filtered MilliQ water, at 50 °C and vortexed until completely solubilized. Prior to sample preparation, all solutions were filtered through a 0.22 μm Filtropur S 0.2 filter (SARSTEDT AG & Co., Germany) to achieve sterility. After this, all sample handling before their respective analysis was performed in a laminar flow hood to maintain sterility and avoid contamination with external factors.

2.3 Characterization of the SLNPs

The different characteristics of a NP, aside from their matrix component, highly influence their properties and subsequent usefulness. Larger particles might limit their ability to cross certain barriers, and their shape and mechanical properties might induce a better penetrating ability. Other examples are also present and must be considered upon NP preparation. Here, the characterization of these SLNPs focuses on their size, charge, morphology and pH.

2.3.1 Size and charge

To assess both size and polydispersity index, as well as the charge, samples were prepared by diluting their respective stock solutions with a 1:100 dilution factor in ultrapure filtered MilliQ water to allow the analysis. SLNPs were diluted to 50 μ g/mL, considering the ATO 5 concentration, and the individual surfactant stock solutions Brij S20 and Monoolein to 150 and 50 μ g/mL respectively. The surfactant mixture was diluted accordingly to simulate the SLNPs solution (Table 2.1). This assay was performed for both batches produced and shipped by the external collaborators as mentioned before.

Table 2.1. Samples analyzed for the characterization assays and their stock and working concentrations. Working concentrations were obtained by diluting the stock solutions in a 1:100 factor in ultrapure filtered MilliQ water.

Sample	Stock concentration	Concentration during assays
Brij S20	15 mg/mL	150 μg/mL
Monoolein	5 mg/ mL	$50 \mu g/mL$
Brij S20:Monoolein mixture	15:5 mg/mL	150:50 μg/mL
SLNP solution	5 mg/mL	$50 \mu g/mL$

These samples were then analyzed in a Zetasizer (Malvern Panalytical Ltd., United Kingdom), loading them into disposable folded capillary cells DTS1070 (Malvern Panalytical Ltd., United Kingdom) at the Biointerfaces and Nanotechnology facility at i3S. This characterization allows for the determination of NPs average size (z-average), analyzing the hydrodynamic diameter of particles in a colloid solution, assessing the scattered light associated with their Brownian movement, thus being denominated dynamic light scattering (DLS). This technique also allows for the differentiation between NPs, conferring the polydispersity index (PdI), a measurement of their variability in size and distribution in solution. Finally, the same equipment also allows to assess the surface charge of these particles (zeta potential) by applying an electric field into the sample and analyzing the mobility of these particles in the colloidal solution [71,72].

2.3.2 Transmission Electron Microscopy

There are different techniques to assess the morphological shape of NPs, however, in this work, their shape was assessed by transmission electron microscopy (TEM).

Prior to their examination, SLNP solution was again diluted to the same concentration as described in the previous topic and $10~\mu L$ was mounted on Formvar/carbon film-coated mesh nickel grids (Electron Microscopy Sciences, United States of America), which after 2 min the excess liquid was removed with filter paper. After this fixation step, SLNPs were negatively stained by adding $10~\mu L$ of

uranyl acetate 1% to the grids. Samples were again left for another 10 seconds, removing the excess liquid with filter paper. After these steps, sample characterization was carried out using a JEOL JEM 1400 TEM at 80 kV (Tokyo, Japan) and the pictures were taken with a CCD digital camera PHURONA, EMSIS Germany at the Histology and Electron Microscopy facility at i3S.

Analysis was performed for the surfactant solutions, as described in Table 2.1, and the sample preparation for TEM analysis was then repeated.

2.3.3 pH assessment

To assess solutions pH, NPs were diluted in ultrapure filtered MilliQ water to the previously mentioned concentration, $50~\mu g/mL$, and the pH was measured using a pH-meter SevenDirect SD20 (Mettler Toledo, New Zealand). The respective surfactant solutions were also prepared as described in Table 2.1 and pH was measured as mentioned above.

2.3.4 SLNP fluorescence quantification

Track and visualise NPs in a cellular context is technically demanding. For this, is common to label NPs with fluorescent dyes, e.g. example FITC, that absorb and emit light at precise wavelengths, fundamental to localize them under a fluorescence detection (laser or lamp). The first step was to perform a calibration curve with SLNPs serial dilutions.

The fluorescently labelled SLNPs were serially diluted from the stock solution to the concentrations 1000, 500, 50, 0.5, 0.05, 0.025, 0.010, 0.005, 0.0025, 0.001, 0.0005, 0.0001 μ g/mL in ultrapure filtered MilliQ water. Dilutions were also performed using Endothelial Basal Medium 2 (Lonza Group Ltd., Switzerland) (EBM-2) with 0.5% Fetal Bovine Serum (FBS), both from Quimigen, Portugal. Then, these solutions were placed in black 96-well microplates (Greiner Bio-One International GmbH, Austria) with a transparent bottom to allow fluorescence intensity measurement with a Synergy Mx microplate reader (Agilent Technologies Inc, USA). With the results, a calibration curve with the different concentrations of SLNPs and their fluorescence intensity was drafted [73].

2.4 Stability assessment of SLNPs

The assessment of SLNPs stability was performed by incubating the NPs for different periods of time under different conditions to mimic physiological conditions. Samples were first diluted to the concentration of 50 μ g/mL using different dispersants: ultrapure filtered MilliQ water and EBM-2 supplemented with 0.5% FBS. This serum concentration was used as a means of simulating the *in vitro* environment in which endothelial cells used in this work will be incubated with the SLNPs [74]. For the samples diluted in water, samples were incubated at different temperatures in a water bath (room temperature ~25 °C and 37 °C) to assess temperature effect and the samples in EBM-2 culture media were incubated at 37 °C to assess the effect of the dispersant in their stability.

For size and charge characterization, the different samples were incubated for 30 min, 1, 3, 6, 24, 48 and 72 h, assessing the stability and characteristics over time. These measurements were performed under the same technical conditions as the normal characterization described in the previous topic (2.2.1 Size and Charge) with the slight change that the instruments temperature was increased to 37 °C when performing the measurements of the samples incubated at this temperature. Due to the lack of compliance with the Zetasizer quality standards for result interpretation, obtained by measuring the surfactant solutions prepared for the SLNP characterization, these samples were not further tested for stability assessment with this equipment. Also, due to other device limitation, it was not possible to correctly measure the charge of the NPs incubated in EBM-2, as the culture media has a considerable number of ions and salts in its composition. These ions damage the electrodes of the measuring cell, yielding random and uncorrelated results. For this assay, three independent assays with three internal replicates were performed for each batch.

SLNPs morphological characterization was also performed with the same solvents and incubation conditions, however, samples were only measured in the beginning (0 h) and after 72 h of incubation in each condition. To further simulate the stability of this colloidal solution simulating *in vivo*

administration, SLNPs were also diluted to the same concentration in mouse cerebrospinal fluid (CSF) obtained from a collaboration with Dr. Isabel Cardoso from the Molecular Neurobiology Laboratory at i3S. Since CSF extraction from the mouse brain only yields a very small amount of fluid (\sim 2-6 μ L per animal), this condition, as a preliminary study, was not possible to be performed over different periods of incubation. These TEM studies also allow for the identification and assessment of protein corona formation. This is a structure that is formed by coating the surface of NPs with different sets of proteins and other molecules and negatively influence the efficacy of the nanosystem. Different types of corona can be formed, a dynamic and reversible with low affinity coating (soft corona) that will eventually lead to a more stable and strong bound hard corona. This layer of proteins will decrease the blood circulation time of NPs, hinder their uptake and targeting by the desired tissue and ultimately lead to their premature clearance from the body, thus, assessing possible corona formation would be a way to check the maintenance of the stable properties of these SLNPs [75,76].

To assess the pH of the sample and possible variations that could compromise the appropriate function of the SLNPs, these were diluted in the previously mentioned conditions (in ultrapure filtered MilliQ water incubated at RT and 37 °C and in EBM-2 complemented with 0.5% FBS. The pH was measured for incubation periods of 6 and 72 h. Variation assessment was also performed for the surfactant solutions, individually and mixed, as described in Table 2.1.

2.5 Cell culture preparation

To simulate the effect of our SLNPs on eukaryotic cells, different *in vitro* models arise. For BBB reproducibility the transwell system is the most common approach, but for more simpler assays such as the determination of cell viability and cytotoxicity of the system, a simple *in vitro* culture of cells was performed.

In this work, *in vitro* assays were performed using hCMEC/D3 (Cedarlane Laboratories Limited, USA), as these are easy to work with and used as a standard cell line for *in vitro* BBB model preparation. For culturing the cells, the appropriate media for seeding and growth must be prepared fresh. For hCMEC/D3 EBM-2 media was supplemented with 1% Penicillin Streptomycin (Pen Strep) (Gibco, USA), 5% of FBS, hydrocortisone (Merck KGaA, Germany), ascorbic acid (Merck KGaA, Germany), HEPES (Gibco, United Kingdom), and bFGF (PeproTech, Inc., United Kingdom) at final concentrations of 1.4 μ M, 5 μ g/mL, 10 mM and 1 ng/mL respectively. The medium was also completed with chemically defined lipid concentrate (Gibco, United Kingdom) in a 1:100 dilution and before cell seeding the surface of the seeding platform, either a multiwell plate or a T-flask, is firstly coated with a solution of Collagen Type I (Merck KGaA, Germany) at 150 μ g/mL for 1 h to allow for the appropriate attachment and growth of these cells [74].

The cells used in this work were cryopreserved in FBS with 10% of dimethyl sulfoxide (DMSO) (Merck KGaA, Germany), a cryopreserving agent that prevents crystal formation inside the cells, which otherwise would lead to the burst of the cell membrane. So, to thaw them, already described protocols were adapted [74]. Briefly, in a laminar flow hood, a T-flask (SARSTEDT AG & Co., Germany) was coated with collagen Type I with enough volume to fill the bottom and left to incubate at 37 °C with a 5% of CO₂ supply for at least 1h. After that, the excess collagen was removed, and the T-flask washed with warm 1X Phosphate-Buffered Saline (PBS) (Gibco, United Kingdom). The bottom of the T-flask was filled with EBM-2, maintaining it moisturized. After that, cells were thawed and quickly diluted in the same medium to prevent harmful effects that DMSO has towards them at RT. Cells were centrifuged in a Centrifuge 5804 R (Eppendorf SE, United Kingdom) at 1200 rpm for 8 min and the supernatant was discarded. The cell pellet was then resuspended in EBM-2 and inserted into the T-flask and left to incubate at 37 °C with a 5% CO₂ supply (BINDER GmbH, Germany), changing the media every 2-3 days. When reached a confluent state, cells were subcultured following a very similar protocol as the one described above. For that, the medium in the T-flask is removed and the container washed with warm 1X PBS to remove residual FBS. After this, enough trypsin 0.25% EDTA (Gibco, Canada) solution to fill the bottom of the T-flask is added and incubated at 37 °C with 5% CO₂ supply for ~4 min. Cell detachment was controlled and verified under optical microscope (Olympus LS, Japan). After this incubation the trypsin is blocked by adding previously warmed EBM-2 with 5% FBS, resuspending the cells and transferring them to a 15 mL centrifuge tube. These are again centrifuged at 1200 rpm for 8

min, after which the supernatant is discarded and the pellet resuspended in the appropriate medium, depending on the desired use, either to cryopreserve them, re-seed them on other T-flasks for expansion, microplate wells, etc.

2.5.1 MTT solution preparation

Before performing the assay, 3-(4,5-Dimethyl-2-thiazolyl)-2,5-diphenyl-2H-tetrazolium Bromide (MTT) aliquots were prepared [77]. For that, 100 mg of MTT (Merck KGaA, Germany) was weighted and solubilized in 20 mL of 1X PBS, to a final stock concentration of 5 mg/mL stored at -20 $^{\circ}$ C.

2.5.2 SLNP cytotoxicity

The assessment of the cytotoxic effect of SLNPs was carried through the MTT assay. Prior to that, hCMEC/D3 cells were seeded on 96-well microplates (SARSTEDT AG & Co., Germany). The wells of these microplates were previously coated and seeded following the previously mentioned steps regarding cell culture preparation, seeding each well with approximately 10 000 cells in EBM-2 with 5% FBS.

The 96-well microplates used for the MTT assays contained four different types of groups: the control, where cells were seeded and incubated in normal culture conditions; one with the condition being studied; cells incubated with the vehicle, mimicking the environment of the substance being tested, i.e., for SLNPs this was considered to be water; and the final one containing all the acellular controls of the ones just described.

For this purpose, a cytotoxic concentration curve was prepared to determine the desired concentration to administer to cells when considering internalization and permeability assays. For that, SLNPs were serially 10-fold diluted (50 to $0.005~\mu g/mL$) in EBM-2 supplemented with 0.5% FBS (Table 2.2: I-V). A surfactant range was also assessed in this study, as the excess of surfactant present in solution might induce some cytotoxicity. For that, a surfactant mix stock solution was prepared in the same way as described in **2.2 Surfactant solution preparation** and from that, the same serial dilutions were performed, mimicking the SLNPs concentrations (Table 2.2).

Table 2.2. Surfactant mix (Brij S20:Monoolein) and SLNP solution concentrations tested for cytotoxicity studies in hCMEC/D3 cell line.

Solutions I-V	were prepared by	v serial dilutions	starting from	the Stock solution.

	Concentration (μg/mL)					
Sample	Stock solution	I	II	III	IV	V
Brij S20:Monoolein	15000:5000	150:50	15:5	1.5:0.5	0.15:0.05	0.015:0.005
SLNP solution	5000	50	5	0.5	0.05	0.005

The cell culture medium of the previously seeded wells was replaced by these prepared samples, with the respective control containing only EBM-2 supplemented with 0.5% FBS. After this, the cells were incubated for 6 h at 37 °C with a 5% CO₂ supply, after which these described solutions were removed and substituted with a MTT solution [77]. This MTT solution was prepared by diluting the previously prepared 5 mg/mL aliquots in EBM-2 supplemented with 0.5% FBS to a final concentration of 0.25 mg/mL. The multiwell plates were left to incubate under the same conditions for another 3 h protected from the light, after which, this media was again removed and substituted with ethanol 100% (Honeywell International Inc, Charlotte, USA). These plates were then measured in a Synergy Mx microplate reader, assessing the absorbance values at 570 nm and 630 nm.

Despite a preference to use hCMEC/D3 cells, as these mimic the BBB, the assessment of SLNPs cytotoxicity in other cells might rule out a possible susceptibility of this cell line. For this, medulloblastoma cell line (DAOY, ATCC HTB186, USA) was cultured and the effect of the higher SLNP

concentration (50 μ g/mL) was re-assessed. This concentration was chosen after crossing information between the previous assay and different research articles, assessing concentrations of ATO 5 based SLNPs within this range, without signs of cytotoxic response [67,78,79]. For culturing these cells, Dulbecco's Modified Eagle Medium (DMEM) (Gibco, United Kingdom) with 1% L-Glutamate, 1% Pen Strep and 10% FBS was used. Similar as described for hCMEC/D3, DAOY cells were thawed and incubated in the same conditions, with the appropriate medium [80]. When confluent, cells were subcultured into 96-well microplates, seeding 10 000 cells per well in DMEM (10% FBS). After 24 h of incubation under the same conditions, SLNPs solution was prepared in DMEM supplemented with 0.5% FBS. The wells of the microplate had their medium changed, repeating the same procedure previously described. After 24 h of incubation another MTT sample was again prepared and the following procedure repeated.

After evaluating the toxic effect of the SLNP solution, other MTT assays were performed, however testing lower concentrations of SLNPs (5 and 500 ng/mL). For that, hCMEC/D3 cells were seeded in 96-well microplates as described above. After administering SLNPs samples, the plates for both concentrations were left to incubate at 37 °C with a 5% CO₂ during different time periods (6, 24, 48 and 72 h). After incubation, the MTT solution was again freshly prepared, and the procedure described above was repeated for each plate.

2.5.3 Optimal surfactant range

With the possibility of there being no SLNPs present in the previously tested solutions, the focus shifted to trying to identify possible components in the mixture that could be causing a toxic effect, as well as determining its appropriate concentration for cell culture assays. For that, individual surfactant stock solutions were prepared as previously described and diluted at different concentration ranges in EBM-2 with 0.5% FBS. Brij S20 was serially diluted to 150, 100, 50, 5 and 1 μ g/mL while Monoolein was serially diluted to 50, 5 and 1 μ g/mL. These were administered to cells plated in 96-well microplates as described and incubated for 6 h at 37 °C with 5% CO₂. After the incubation period, the MTT solution was again prepared, and the cytotoxicity procedure was repeated.

After determining the most appropriate concentrations, a surfactant mixture stock solution was prepared considering the dilution factors with a final concentration of Brij S20:Monoolein of 0.5:5 mg/mL. For that, two intermediate solutions were prepared, one containing 1 mg/mL of Brij S20 and another with a concentration of 10 mg/mL of Monoolein and 500 μ L of each solution were mixed. Afterwards, serial dilutions were made in EBM-2 with 0.5% FBS, achieving the concentrations of 10:100, 5:50 and 1:10 μ g/mL of Brij S20:Monoolein. These samples were then presented to hCMEC/D3 cells seeded one day before in 96-well microplates. Another MTT assay for the incubation of 6 h was performed as described before.

2.6 Cell internalization assays

To assess hCMEC/D3 ability to uptake SLNPs, two technical approaches were taken: Fluorescence activated cell sorting (FACS) and confocal microscopy.

2.6.1 Flow Cytometry - FACS

For FACS analysis, hCMEC/D3 cells, previously in culture, were subcultured into 24-well plates (SARSTEDT AG & Co., Germany) previously coated with collagen Type I for 1 h. In these plates, 60 000 cells/well were seeded and incubated in EBM-2 with 5% FBS for 24 h prior to SLNP treatment at 37 °C with 5% CO₂ supply. SLNPs were diluted in EBM-2 with 0.5% FBS to reach a final concentration of 500 ng/mL, which was then administered to cells by removing the pre-existing culture medium and substituting it with this sample. The control of cells untreated with SLNPs was also performed. Plates were then incubated for 4 h, after which, each four wells for condition were trypsinized following the previously referred protocol, cells placed into 15 mL centrifuge tubes and centrifuged for 8 min at 1200 rpm. Afterwards, supernatant was discarded, and the cells were resuspended in 300 μ L of PBS (1X). This was performed for three independent assays each with four internal replicates [81]. Cells

were analyzed by FACS using a BD Accuri 6 machine (BD Biosciences, United States of America) at the Translational Cytometry facility at i3S. Gates were set up to acquire 100 000 events for each condition.

2.6.2 Confocal microscopy

Due to technical issues, plastic 24-well plates are not suitable for confocal analysis, so, hCMEC/D3 cells were seeded on top of glass coverslips (Auxilab, Spain). To maintain the sterility of this process, these coverslips were first washed in ultrapure filtered MilliQ water at room temperature under continuous mild agitation, after which the solvent was changed to absolute ethanol and the agitation process repeated. After this washing step, the coverslips were left to dry and autoclaved before culturing cells. The coverslips were coated with collagen Type I and the seeding procedure was repeated, seeding 10 000 cells per coverslip. After 24 h of incubation, the culture medium was changed with EBM-2 with 0.5% FBS. To three coverslips this medium did not contain SLNPs, however, the other three coverslips were supplied with 500 ng/mL of SLNPs previously diluted in the medium. After 4 h of incubation, cells were fixed with paraformaldehyde (PFA) [82]. For this step, the culture medium in which they were incubated was removed and the coverslips were washed carefully with PBS (1X) to remove the non-adherent SLNPs. Afterwards, 2 mL of PFA 4% (v/v), (Frilabo II, Lda., Portugal), were added filling the well and submerging the coverslip and incubated for 15 min. PFA was then removed, and the coverslips carefully washed with PBS (1X) three times for 15 min each. Finally, the coverslips were stored at 4 °C in PBS (1X) until characterization.

For cell staining, well described protocols were adapted [82]. Briefly, the coverslips were first washed with PBS (1X) three times for 10 min each time and a Triton X-100 (Fisher Scientific, Portugal) 0.2% (*ν/ν*) in PBS (PBS-T 0.2%) was prepared and added until the coverslip was submerged. This solution was used to permeate the fixed cells and allow for the nucleus staining. After 10 min, the PBS-T 0.2% solution was removed and the coverslips were incubated with a pre-prepared DAPI (Merck KGaA, Germany) solution, with a concentration of 33 μg/mL, for 30 min, that allow for the cell nuclei staining. After, the coverslips were again washed three times with PBS (1X) for 10 min each, to remove excess of DAPI solution, and then incubated with F-actin solution for 15 min (Invitrogen, United States of America) at RT. The F-actin solution stains the cell cytoskeleton molecule actin with a red colour and was prepared by diluting the stock solution to a final concentration of 1 μM. After F-actin incubation the coverslips were washed again with 1X PBS and mounted on the microscope slide with ProLongTM Glass Antifade Mountant (Invitrogen, United States of America). Samples were analyzed using a Confocal Leica SP5 microscope (Leica Microsystems, Germany) at the Bioimaging facility at i3S.

2.7 Statistical analysis

Statistical analysis performed on the data presented in this work was obtained by using Prism 9 (GraphPad), applying ANOVA statistical analysis and paired T-Student tests when applicable. Significance levels are considered as * for p < 0.05, ** for p < 0.01, *** for p < 0.001, **** for p < 0.001 and ns for p > 0.05. The results were reported as mean \pm standard deviation (SD).

RESULTS AND DISCUSSION

3.1 Characterization of the SLNPs

3.1.1 Size and charge

The size of the NPs will highly influence the functionality of the delivery system, playing a key role in assessing their stability in solution, with larger NPs possibly compromising the applicability [64,83,84].

The size characterization of these SLNPs was assessed for both batches (Table 3.1) and the first evidence is the massive size difference between the different batches and conditions. The Batch #1 had double the diameter (103.69 ± 3.18 nm) compared to the second one (56.39 ± 0.78 nm). A possible explanation for this is related to their shelf life, as the second one was freshly prepared for these experiments while the first was already produced and stored for a considerable period. Researchers have addressed the stability of different nanosystems over periods of time in different storage conditions, as different parameters influence the characteristics of NPs [85–89]. Depending on temperature and pH, most lipidic NPs are ultimately preserved by freezing or freeze-drying processes, however, when performing these steps, one should take into account the chemical elements present in the different formulations and the possible polymorphic transitions. Since the production process of the SLNPs used in this work heavily relies on these transitions, taking advantage of cooling and heating cycles to fragment oil into these NPs, these preserving processes are not an option. In fact, researchers have also addressed the fact that surfactants and emulsifiers with lower melting points than the NPs oil phase might work as a catalytic NP nucleus forming agent, creating further smaller SLNPs and thus altering the stability and properties of the original solution [87,89,90].

Another important point to highlight is the somewhat high polydispersity of these SLNPs. The PdI values give a measurement of the heterogeneity of the sample, which also influences the stability and response of the system. Having a more polydisperse solution could lead to unexpected behaviour of the system [91]. It also serves as a measurement of the stability of a colloid system, since an increase in PdI might be associated with the destabilization and aggregation processes occurring in the sample. However, since the production procedure heavily relied on the cooling, heating and fragmentation of larger clusters into smaller particles, a moderate PdI becomes an artifact of the production process, rather than an indicator of a loss of stability, especially if it is impossible to control the size of the fragments produced, as it is in this case.

Table 3.1. SLNP and surfactant samples characterization, assessing Size, PdI, Zeta Potential, Shape and pH.

Values are presented as mean \pm SD from three independent assays with three replicates each.

^{*} Shape of the samples can be assessed in next images regarding TEM analysis.

Sample	Size (nm)	PdI	Zeta Po- tential (mV)	Shape	Solution pH (± 0.01)	Meet Quality Criteria
SLNP Batch #1	103.69 ± 3.18	0.28 ± 0.02	-16.82 ± 0.69	Spherical	4.39	Yes
SLNP Batch #2	56.39 ± 0.78	0.29 ± 0.02	-9.80 ± 0.82	Spherical	5.18	Yes
Surfactant mixture	21.32 ± 1.12	0.59 ± 0.02	-2.37 ± 0.71	Irregular*	8.46	Yes
Brij S20	99.89 ± 85.24	0.47 ± 0.08	-2.14 ± 0.58	Spherical	8.78	No
Monoolein	889.80 ± 103.00	0.32 ± 0.07	-15.0 ± 2.01	Irregular	8.99	No

The charge of these formulations also influences the usefulness and stability aspects. Positively charged NPs might interact with cells more easily since these have an overall negative surface charge [92–94]. The SLNPs assessed in this study appear to have a slightly negative charge (-16.82 \pm 0.69 mV for batch#1 and -9.80 \pm 0.81 mV for batch#2) as depicted in Table 3.1. This might be a consequence of the chemical interactions between ATO 5 molecules and the solvent, resulting in proton (H⁺) release to the environment decreasing its pH and rendering an overall negative charge to these SLNPs. This characteristic however also prompts for a better stability of the system. Not only are the SLNPs coated in their surfactant layer, comprised of Brij S20 and monoolein, which avoids their coalescence and maintains their stability, but researchers have addressed the fact that charge also plays a key role in preventing post production SLNP aggregation and system destabilization, with the more extreme zeta potentials (+/- 30 mV) resulting in a more stable solution than those closer to zero [95,96].

On the other hand, the surfactant mixtures also yielded interesting results. Monoolein and Brij S20 solutions, by themselves, do not appear to qualify for analysis in this equipment, as for one the entities present are too large to be quantified and for the other, the sample is too polydisperse. According to the literature, Brij S20 has a critical micellar concentration (CMC) of 0.069 mM (22 μ g/mL) [97]. Since the working conditions for the production of the surfactant sample had an initial concentration of 15 mg/mL, Brij S20 is highly likely to be forming micelles in this solution, whose size cannot be controlled, resulting in this high polydispersity, and consequent artifacts of the readout. As for monoolein, as will be further addressed in the next section, this surfactant seems to organize itself in larger structures, falling outside the measuring boundary of the device.

When analysing the surfactant mixture however, data from Appendix A1 seems to highlight the presence of the two populations, one regarding the Brij S20 solution with the smaller sizes (14.70 ± 0.28 nm) and the other for the Monoolein with the larger size (1238.00 ± 45.01 nm). These results might suggest that the two surfactants do not interact, creating their own separate entities, with Brij S20 creating micelles and monoolein another kind of structure, as will be highlighted in the next section. Despite not being able to quantify the charge of the surfactant samples, as these do not fall in the machine reading quality criteria, the surfactants are expected to remain neutral, with the SLNP charge being associated with the ATO 5 present in the particles.

3.1.2 Morphology

Nanoparticle shape is a very important issue consider when characterizing these formulations, as different specific shapes might induce different cell/host responses, as well as for different post-production treatments requirements [98].

In this case, as can be seen in Figure 3.1, these SLNPs appear to have a round shape in both batches. This trait of the SLNPs can be considered as a result of the success of the nucleus formation during production cycles [70]. It is also important to highlight the differences between batch sizes, again as a possible result of the shelf-time the first batch already possesses when compared to the second batch. Another interesting point in these images is the darker stains present in the samples where the SLNPs reside. These are also present in all samples containing monoolein, suggesting that this surfactant is creating different phases, specially the one where the SLNPs are present. On the other hand, Brij S20 samples only resemble the small dots, possibly micelles with varying sizes, as can be seen [97]. These entities, unfortunately, are not present with a single size, but rather Brij S20 organizes itself in micelles with various sizes, some bigger than the SLNPs, other smaller, which not only hampers the isolation of the NPs, removing the excess surfactants, but also introduces artifacts in the SLNP images, making the distinction between SLNPs and Brij S20 micelles a challenge. When looking at the surfactant mixture, it is also possible to see the presence of the small dots inside the dark stains, further indicating the possibility that Brij S20 does not interact with the monoolein in solution, but rather interacts with itself forming the micelles seen throughout the different samples that contain this component.

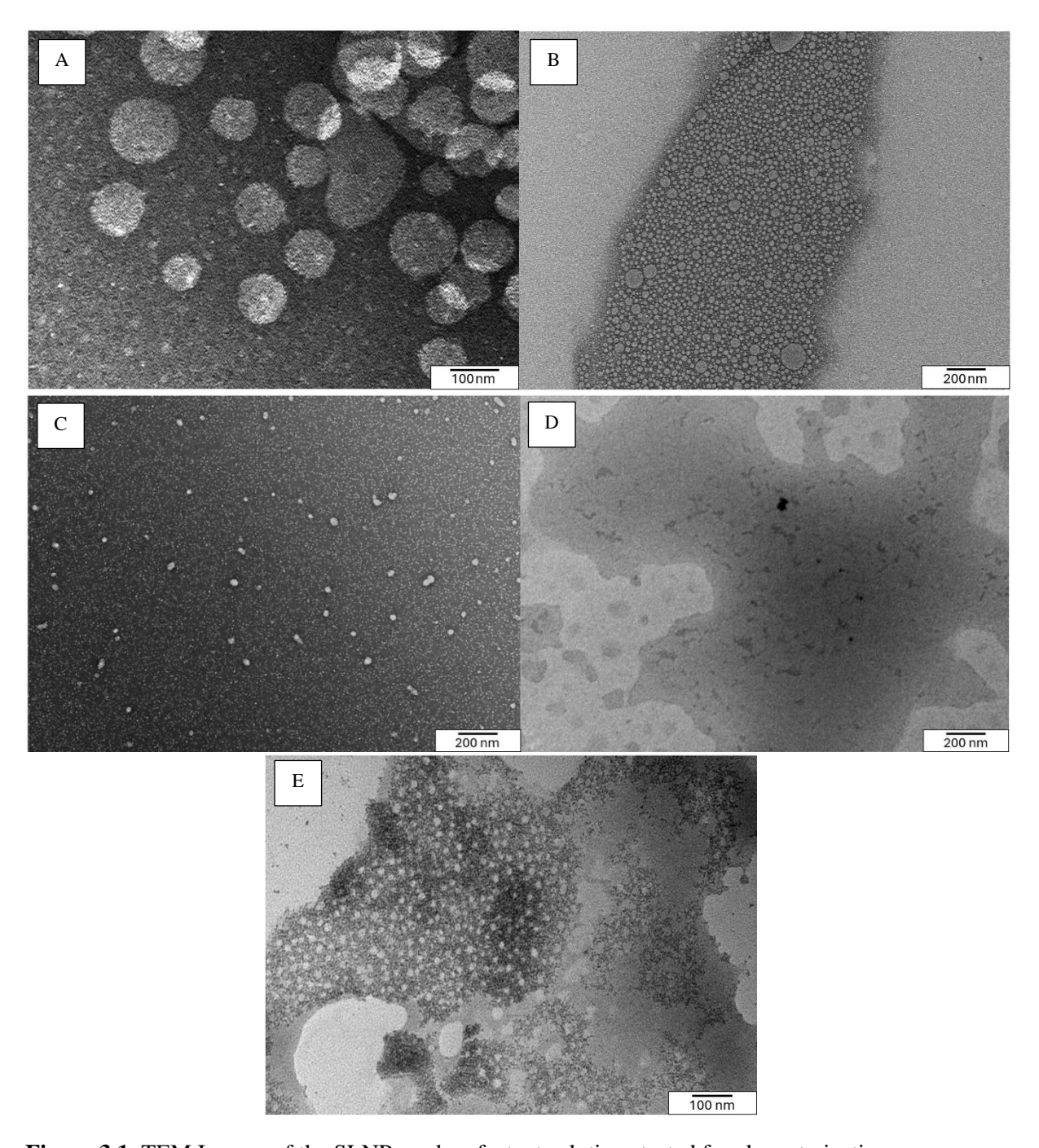


Figure 3.1. TEM Images of the SLNPs and surfactant solutions tested for characterization. (A) SLNPs from Batch#1; (B) SLNP solution from Batch#2; (C) Brij S20 Solution; (D) Monoolein Solution; (E) Surfactant Mixture.

These results highlight the spherical shape of the SLNPs, confirming the size differences between batches and highlighting the Brij S20 micelle formation. It also highlights the irregular shapes formed by monoolein and the absence of interaction between the two surfactants when incubated together.

3.1.3 pH

The pH is another important factor in the solution of the NPs produced. As an example, it is described, that the pH can greatly influence the zeta potential of the NPs and induce their destabilization and aggregation [99,100]. Not only this, but the human body presents different pH values across

different organs and tissues, thus, assessing the pH of the solution in both stable and unstable conditions must be done to better confirm the applicability of the formulation.

As can be seen in Table 3.1, SLNP solution appears to have an acidic pH. The different surfactants used however do not show signs of being able to change the pH by themselves, as these components can only be ionized by water in their alcohol groups. This reaction however is characterized by a pKa \sim 14-16, meaning that at these conditions, and at a pH of 5.18 \pm 0.01, it is very unlikely that the surfactants are being ionized by water molecules [101,102]. On the other hand, ATO 5 is mainly composed of palmitic and stearic acids (C16 and C18 saturated carbon chains). These molecules present pKa \sim 4.5, above which they are ionized by water and release protons to the environment. This reaction results in the low pH observed for SLNP samples and might be a probable reason for the negative charge of the SLNPs presented in Table 3.1 [103].

3.1.4 Fluorescent intensity

Figure 3.2 represents the fluorescence intensity distribution for the different SLNP concentrations that were evaluated in the assay. One of the most distinct characteristics is the difference between the scaling of the fluorescence units (F.U.) observed between plots. One of the possible explanations for this issue could be related with the solvent used. Different authors have addressed the effects of different solvents on fluorescent probes, reporting both variations in the measured intensity, as well as a shift in the wavelength at which the signal is emitted [104–108]. Associated with this, FITC has also been described as a pH-dependent probe, with its characteristics and fluorescence signal being highly influenced by pH variations [109–111]. Considering the fact that the SLNP solution is prepared in water, which presents an acidic pH, when in EBM-2, a physiological controlled pH, readout variations become expected.

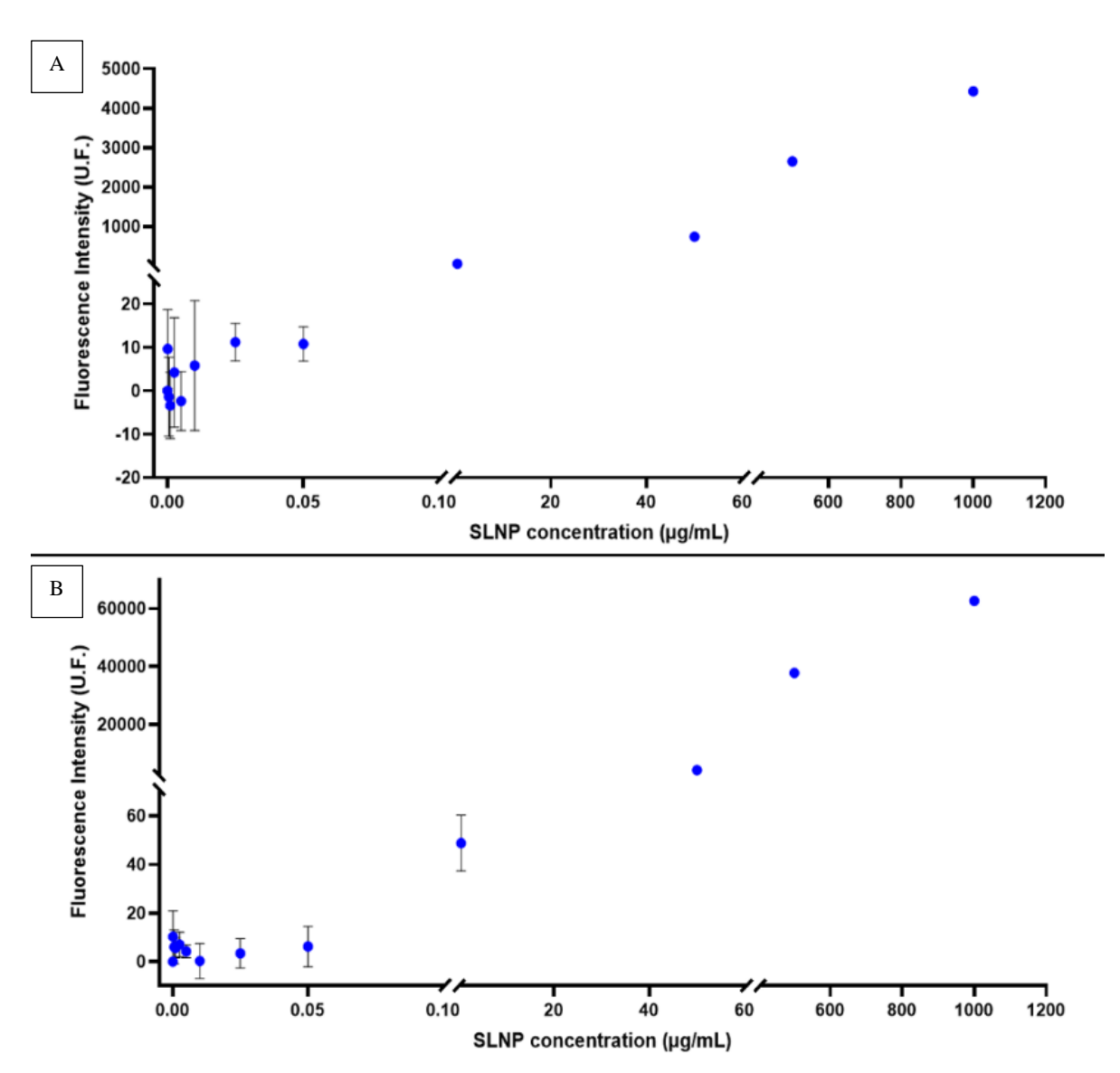


Figure 3.2. Fluorescence intensity of increasing concentrations of FITC-labelled SLNPs (0.0001, 0.0005, 0.001, 0.0025, 0.005, 0.010, 0.025, 0.050, 0.500, 50, 500 and 1000 μ g/mL). (**A**) SLNPs prepared with water as the solvent; (**B**) SLNPs prepared with EBM-2 with 0.5% FBS as the solvent. Values represent the mean \pm SD (n = 5).

Note, some error bars are not shown in these plots as they are too small to be represented at this scale.

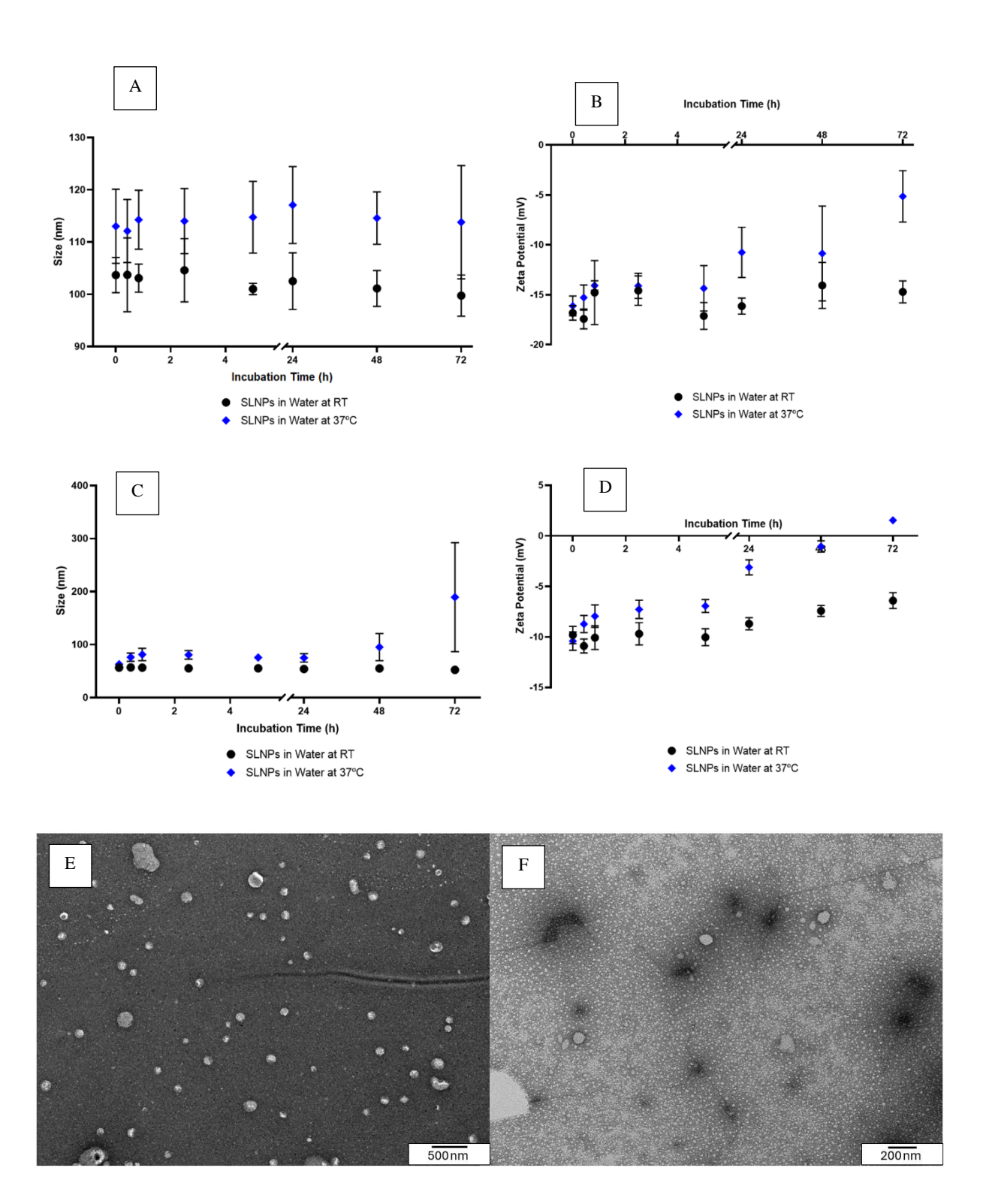
Other than scaling variations, it is also possible to see that there is fluorescence intensity for all the concentrations addressed in this experiment. However, looking at the lower values, it is highly probable that the observed intensity is residual, associated with the background noise of the readings, rather than the values observed for the four higher concentrations. With this in mind, it is possible to see that at the concentration of 500 ng/mL, although low, there is a measurable fluorescent signal. However, the SLNP fluorescence labelling process and its variables should be considered, e.g. yield of staining, the initial and final concentration of FITC on the SLNPs solution, and other factors, that could influence the results and were performed by the collaborators. Since the system is composed of NPs and micelles of Brij S20, which are present in larger number, the readout associated with this lower concentration can be associated with these micelles and their conjugated FITC probes, rather than SLNPs, which might not be present in the solution at all. This results in artifacts of the readings, yielding fluorescent signal, even in the absence of SLNPs, which renders this data as inaccurate, highlighting, for future work, the necessity to remove the excess of surfactant present in solution, as well as the substitution of this fluorescent probe, as authors have already assessed its shortcomings [112].

3.2 Stability of the SLNPs

Since the main goal of the present work would be to cross the BBB both *in vitro* models as well as, ultimately, being useful for humans being administration, this system is required to be functional and maintain its stability and characteristics upon physiological conditions. For that reason, the SLNPs were prepared and treated under different stimuli that could influence these parameters such as temperature and solvent used. The parameters assessed for these stability issues were the same as in the previous topic, size, zeta potential, morphology and pH, thus using the same equipment for measuring.

3.2.1 Effect of temperature in the stability

To simulate the physiological temperature of the human body, samples were incubated for their designated period in a water bath at 37 °C and were then characterized following the previous methods. As can be seen in Figure 3.3A and C, there is a slight increase in the sizes of the SLNPs in both batches when they are incubated at 37 °C. Also, this increase only happened in the beginning of the incubation, as the sizes remain constant throughout the whole incubation period. A possible explanation for this behavior could be associated with the destabilization of the system and its aggregation as has been reported for different systems [113–115]. However, that does not seem to be the case with these NPs. When analyzing the first batch of particles, and by comparing the DLS results with the TEM images (Figure 3.3E, F, G, H, I), one can in fact identify the increased size of the particles, if measured, but this increase is so little and seems to occur as a result of a swelling like behavior of the SLNPs, rather than their aggregation. Since Brij S20 has its melting point at 44 °C and monoolein at 35 °C, by incubating the SLNPs at 37 °C, the temperature increase might be inducing more liquid-like behavior of the surfactants, increasing its fluidity and consequent size, similar to what happens with cell membranes [116]. However, when looking at the second batch, this increase is slightly more significant, possibly since these particles are freshly prepared and could be more susceptible to destabilization than the previous batch. Not only do these SLNPs swell as a consequence of the increase in temperature, but they also form clusters of individual particles. In 2015, Michen et. al. [117] distinguished different stages of stability of NPs, referring to aggregates of particles as their ultimate form of destabilization, and defining clusters as the groups of particles closer together, but still stable enough to be identified as individual entities. Considering this, the analyzed SLNPs incubated at 37 °C do show some cluster formation, possibly since the increase in temperature might be similar to the early stages of the initial production process, possibly inducing a new cycle of fragmentation. However, since the lipid core is not melted due to the temperature being under the ATO 5 melting point (50-60 °C) the process is not carried out, and some clusters appear. Not only this, but by increasing the temperature one might be increasing the kinetic energy of the system, allowing for the particles in the dispersion to collide and further induce this process [113]. Despite this, the particles in solution do come together to create larger structures rather than being fully dispersed in solution, resulting in the emerging peak observed in the higher sizes in the DLS results (Appendix A2), and screening the surface charge of these SLNPs (Figure 3.3B and D), making them appear to have a neutral charge rather than their characteristic negative zeta potential [118,119]. This last factor can also be visualized through the variations over time. Samples incubated at RT (~25 °C) do not appear to have this variation in charge, being overall negative (~ -10 mV). On the other hand, samples incubated at 37 °C do in fact show changes in zeta potential over time, with their charge coming closer to neutrality with the incubation period, possibly as a result of this cluster formation.



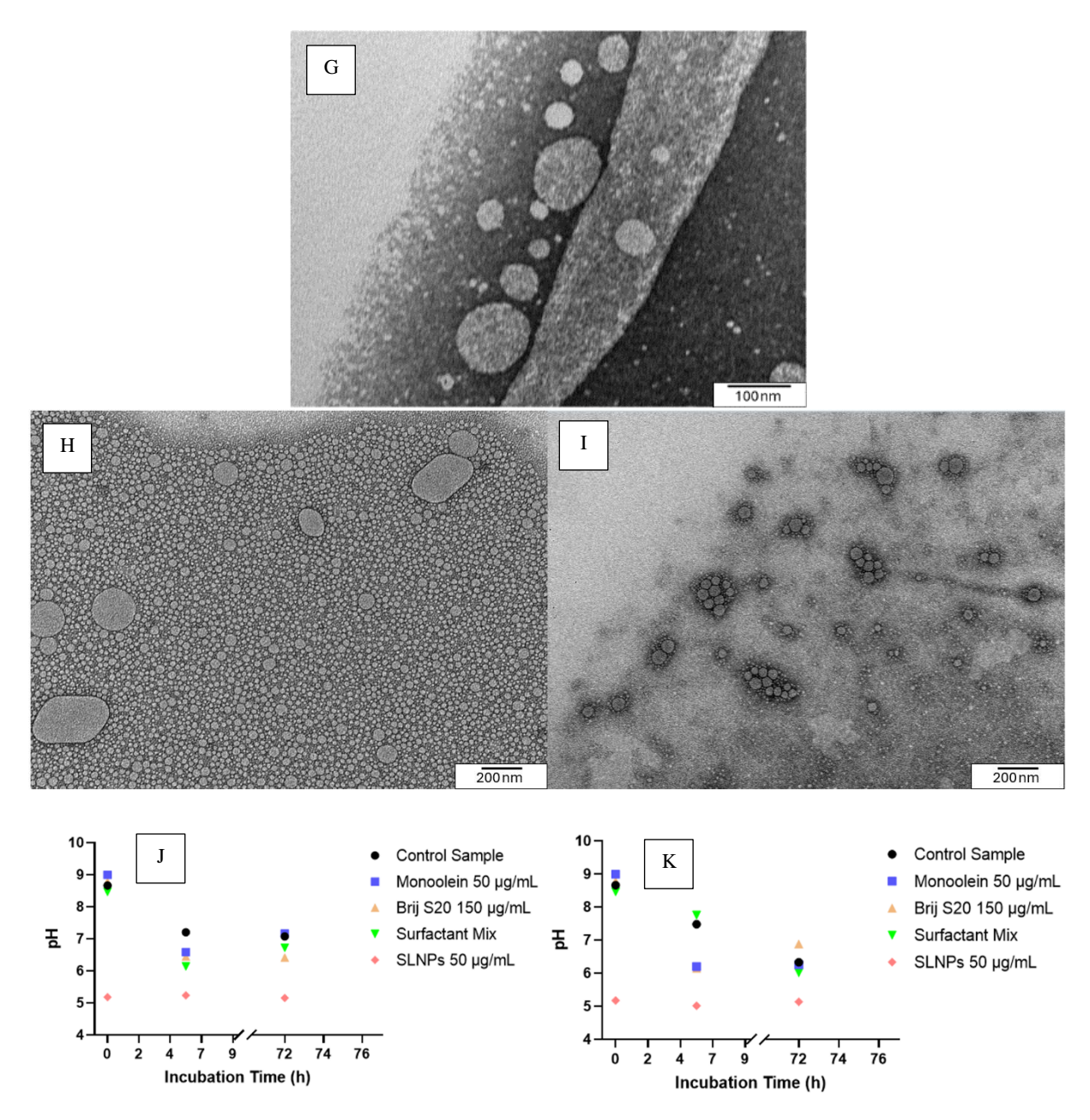


Figure 3.3. Stability assessment of SLNPs (50 μ g/mL) incubated at room temperature (~25 °C) and 37 °C in water throughout time periods of 0 h, 30 min, 1, 3, 6, 24, 48 and 72 h.

(A) Size variations of SLNPs from Batch#1 at both temperatures; (B) Zeta Potential variations of SLNPs from Batch#1 at both temperatures; (C) Size variations of SLNPs from Batch#2 at both temperatures; (D) Zeta Potential variations of SLNPs from Batch#2 at both temperatures; (E) TEM images SLNPs from Batch#1 incubated for 0h (scale bar: 500 nm); (F) TEM images SLNPs from Batch#1 incubated for 72h at 8T (scale bar: 200 nm); (G) TEM images SLNPs from Batch#1 incubated for 72h at 37 °C (scale bar: 100 nm); (H) TEM images SLNPs from Batch#2 incubated for 72h at 37 °C (scale bar: 200 nm); (J) pH variations of SLNPs and their individual components at 8T; (K) pH variations of SLNPs and their individual components at 37 °C. Values represent the mean ± SD and each condition was tested in three independent assays with three replicates each, except for (E-K).

Note, some error bars are not shown in these plots as they are too small to be represented at this scale.

As for the pH characterization, SLNPs tend to maintain their pH over time in both incubation temperatures. As previously explained, the acidic pH results from the ionization interactions between water molecules and the ATO 5. Despite the increase in temperature resulting in cluster formation, water molecules can still pass through the empty spaces between SLNPs and react with the lipidic core maintaining this pH, while the charge gets masked by this effect [101–103,118,119]. Another point to

highlight is the acidification of the control samples over time. As can be seen, both surfactants individually and mixed do not alter the pH of the sample, meaning that their functional groups are not reacting and contributing to the acidification of the environment, rather, this occurs as an artifact since the sample that was measured was always the same, exposing, for every measurement made, the solution to the atmosphere allowing it to react with CO₂, forming carbonic acid, in a reversible reaction, that lowers the pH of the solution [120]. SLNP sample already has an acidic pH, rendering this reaction inefficient and preventing the formation of this compound, thus, maintaining its pH over time.

3.2.2 Effect of the solvent in the stability

When changing the solvent from water to culture media, the results become quite different. EBM-2 culture media is supplemented with FBS in a 0.5% (v/v) concentration, meaning that the proteins present in this solution will further influence the measurements performed. This can be seen in Figure 3.4A and B, since with the increase of time there is a drastic increase in SLNP size. This increase however is not associated with the destabilization of the SLNPs, as can be observed by the acquired TEM images (Figure 3.4C and D) where the particles present themselves with similar sizes to the control. Rather, this change is a consequence of protein-protein aggregation over time, as can also be seen in the TEM images by the large dark stains observed. This causes interferences in the measurements, highlighting the need of a better characterization equipment for these samples. Zeta potential also highlights this need, as it was not measured due to the presence of different salts in the culture media, producing such strong ionic forces that damaged the electrodes of the measuring cell, resulting in randomized uncorrelated values. Another aspect to be analyzed with these experiments is the protein corona formation. Different researchers have addressed the possibility of formatting this coating on different NPs. This is a protection mechanism intrinsic of the host, marking exogenous compounds by binding proteins to their surface, signaling it for engulfment and elimination [75,76,121]. To be successful, NPs and other delivery systems must avoid this process. One way to assess this fact is by studying the size variations of the SLNPs over DLS and TEM analysis. However, proteins in solution, either bound to the surface of the SLNPs or not will be measured and result in the presence of reading artifacts [122,123]. Despite this fact, it is still possible to identify the characteristic size peak associated with the SLNP solution with a size around ~60 nm associated, again, with the heating process of this sample. This suggests that the colloids, despite the increase in temperature and the presence of proteins still maintain their integrity as NPs, without forming aggregates, and without the formation of a protein corona [122,123]. The absence of the corona might result from three sources. One would be the low concentration of serum proteins present in solution. Since the SLNPs are incubated in a solution containing only 0.5% of FBS, these might not be enough to significantly bind to the SLNPs surface and create a significant response. Another possibility is related with the charge of the SLNPs. Most proteins present in the serum are negatively charged, being easily repelled by the SLNPs that have the same polarity [124]. Finally, the most prominent reason would be as a consequence of the surfactants used, specially Brij S20. This surfactant belongs to the polyoxyethylene ether family, possessing PEG residues, notoriously known for their effect on stabilizing NPs and preventing the formation of a protein corona [125–132] This effect can also be seen by the TEM analysis (Figure 3.4C and D), where it is possible to identify the individual SLNPs without a dark mesh around their surface that would represent the corona [123]. Rather this mesh can be visible dispersed in the background, creating artifacts of the reading, but not specifically adsorbed on the SLNPs surface. This fact is also true for the CSF samples, in which the SLNPs were diluted to the same concentrations, yielding the same results as in EBM-2 (Figure 3.4E and F). pH analysis of the EBM-2 samples is represented in Figure 3.4G and H. These results demonstrate that the fact of the SLNPs being incubated in a buffered solution such as this one, ATO 5 with solvent interactions are not sufficient to overpower the buffer capacity of the solvent, maintaining the physiological pH over time and in all samples. This result shows that the acidic pH associated with the SLNP solution would not cause problems when incubated in cell culture and influence cell viability and function [133].

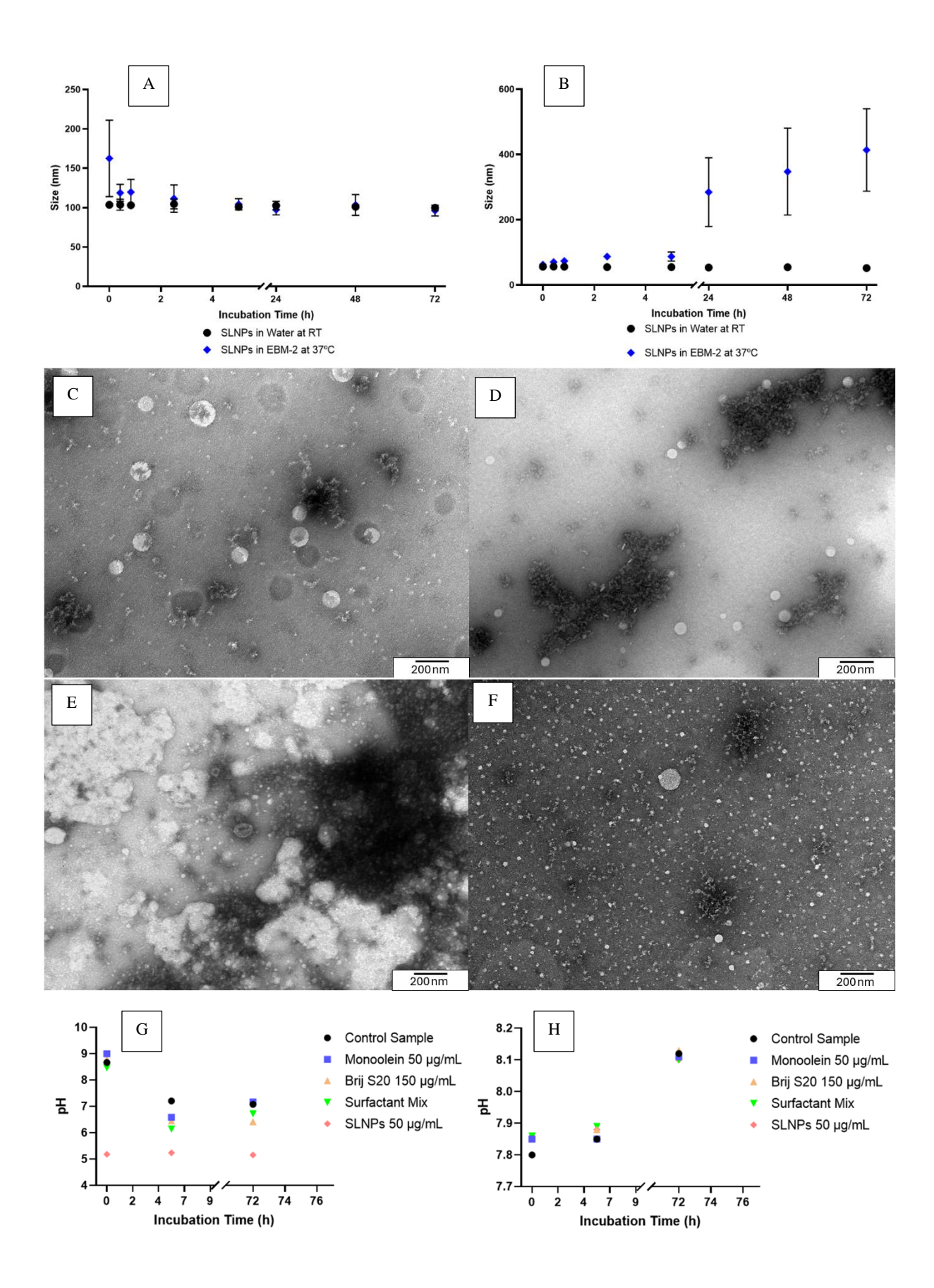


Figure 3.4. Stability assessment of SLNPs (50 μ g/mL) incubated in water and EBM-2 with 0.5% FBS throughout time periods of 0 h, 30 min, 1, 3, 6, 24, 48 and 72 h.

(A) Size variations of SLNPs from Batch#1 in both solvents; (B) Size variations of SLNPs from Batch#2 in both solvents; (C) TEM images SLNPs from Batch#1 incubated for 72h (scale bar: 200 nm); (D) TEM images SLNPs from Batch#2 incubated for 72h (scale bar: 200 nm); (E) TEM images of cerebrospinal fluid (scale bar: 200 nm); (F) TEM images SLNPs incubated in CSF (scale bar: 200 nm); (G) pH variations of SLNPs and their individual components in water; (H) pH variations of SLNPs and their individual components in EBM-2 with 0.5% FBS. Values represent the mean \pm SD and each condition was tested in three independent assays with three replicates each, except for (C-H).

Note, some error bars are not shown in these plots as they are too small to be represented at this scale.

3.3 Cytotoxicity assay

3.3.1 SLNP cytotoxicity

By performing the MTT assay, one might infer about the positive or negative effect the SLNP formulation might have towards the cell viability. This assay is based on the quantification of formazan crystals present that are obtained by the metabolization of the MTT reagent [134,135]. This characterizes the assay as an indirect assessment of cell viability, as what is actually being measured is the metabolic activity of the cells. Considering different reports on the use of SLNPs and the biocompatible characteristics of the different components of these NPs, one might have assumed that there would be no issues with the administration of the system. However, as can be seen in Figure 3.5, that is not the case. When analyzing the range of SLNP concentrations incubated with hCMEC/D3 cells, the deficiency of metabolic activity for higher concentrations is notable. For concentrations above 500 ng/mL cells did not show signs of being metabolic active, presented a change in morphology, were detached, suggesting that these cells appear to be dead. This negative response could be a consequence of different things, one of those being the sensitivity of this cell line to these stimuli. To rule out this hypothesis, a different cell line was incubated with the highest SLNP concentration. Results shown in (Figure 3.6), yield the same outcomes. These suggest that the actual SLNP formulation might be inducing a toxic response in the cells. To counter this effect, two paths can be taken: one could try to identify the most likely agent that is causing this toxicity; on the other hand, the decrease of SLNP concentration should hamper the toxic effect and reduce this negative behavior.

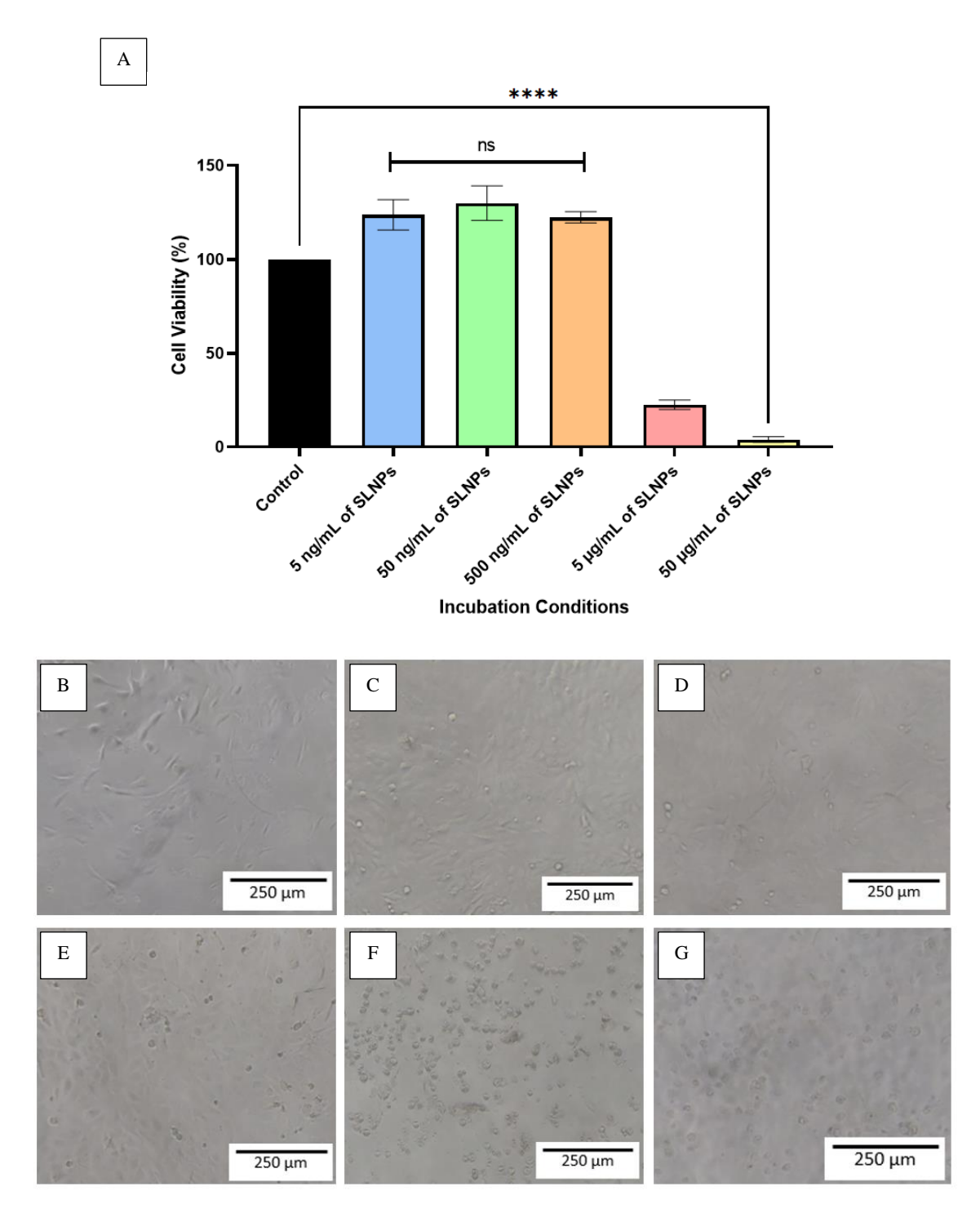


Figure 3.5. Cell Viability assessment of hCMEC/D3 and optical microscopy pictures taken after 6h of incubation with different concentrations of SLNPs.

(A) Cell viability incubated with 0, 0.005, 0.05, 0.5, 5, 50 μ g/mL of SLNPs; (B) Cells incubated with 0 μ g/mL of SLNPs; (C) Cells incubated with 0.005 μ g/mL of SLNPs; (D) Cells incubated with 0.05 μ g/mL of SLNPs; (E) Cells incubated with 0.5 μ g/mL of SLNPs; (F) Cells Incubated with 5 μ g/mL of SLNPs; (G) Cells incubated with 50 μ g/mL of SLNPs. (Scale bar: 250 μ m). Values represent the mean \pm SD (n = 3), except for (B-G).

Changes in cell morphology and detachment observed by the pictures suggest that high concentrations of SLNPs might be responsible for cell death and loss of metabolic activity.

To assess this issue, SLNPs were diluted to the minimum concentration described for the concentration curve (5 ng/mL) and the maximum concentration at which cell viability was high (500 ng/mL) and incubated for different periods of time (Figure 3.7). The results show that, both over the time period and for both concentrations, SLNPs did not show a cytotoxic response, thus considering these promising

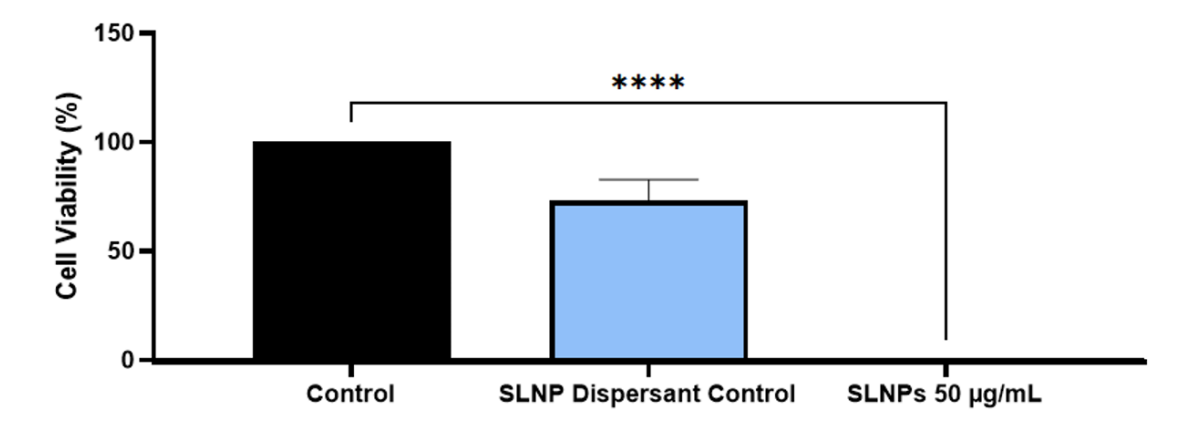


Figure 3.6. Cell viability assay of DAOY cell line incubated with 50 μ g/mL of SLNPs. Values represent the mean \pm SD and each condition (n = 5). These results suggest that the toxicity observed with the SLNP lies within either the formulation or concentration of SLNPs, excluding cell sensibility as a possible issue.

concentrations to work with. However, one must still consider the proportion of surfactants present towards the ATO 5. This might mean that at these low concentrations, not only might the cells being treated with no SLNPs, but rather a solution that would contain low amounts of surfactants, redirecting the work objective to try and identify the possible root of toxicity in this system.

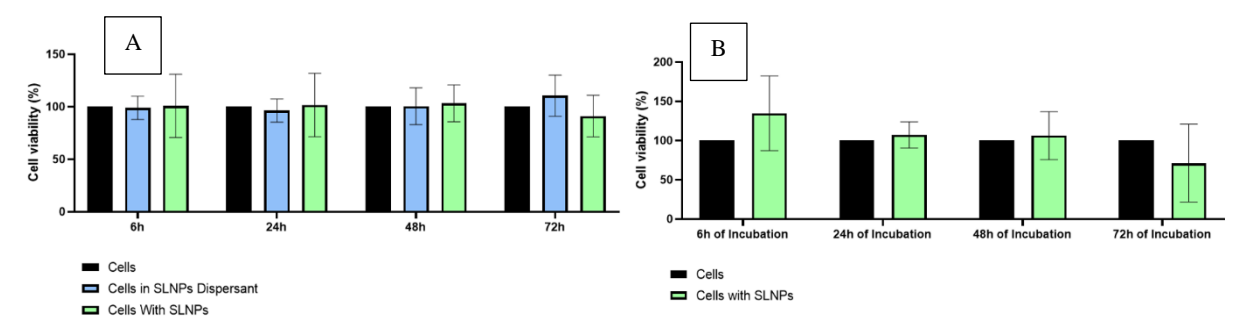


Figure 3.7. Cell viability of hCMEC/D3 incubated with 500 ng/mL (**A**) and 5 ng/mL (**B**) of SLNPs over 6, 24, 48 and 72h.

Values represent the mean \pm SD and each condition was tested in three independent assays with five replicates each. By lowering the concentration of SLNP solution it is possible to mitigate the toxic response ob-served for higher concentrations, however such low concentrations might be associated with the loss of SLNPs entirely from solution.

3.3.2 Cytotoxic agent identification

To identify the possible source of cytotoxicity of this formulation, the different components that comprise it were tested individually with hCMEC/D3 cells, aside from ATO 5. This component was not assessed due to a variety of factors, one of which being its low solubility in aqueous solutions, with its potential solvents being the likes of chloroform [136]. However, if this solubilization was carried out, when the ATO 5 would be incubated in cell culture media, the sample would form different phases as these solvents are not miscible with one another, resulting in the inefficacy of this assay [137]. Despite this, different authors have already addressed the effects of ATO 5 based nanosystems, specifically with the higher concentrations described in this work, concluding that this component does not induce toxicity issues [67,78,79,138]. Not only this, but ATO 5 has already been accepted by the Japanese Standard of Food Additives, which makes this component likely not to be the cause of the toxicity problem [78]. In fact, as observed in Figure 3.8, it is possible to verify that the cytotoxic response described in the previous topic seems to be associated with the surfactants used, more precisely with Brij S20. This might be a consequence of the high concentration used for the preparation of the SLNPs, as this surfactant is present in triple the amount of the lipidic core or monoolein. This results in the micelle formation previously described, rendering the purification of the SLNPs inefficient, again, as these exist with sizes

smaller, equal and bigger than the NPs. Due to this, there will be an excess of surfactant in solution, unbound with the SLNPs that might be interacting with the cells and inducing toxic effects. This concentration of Brij S20 might be too high for cell culture, resulting in possible cell membrane permeabilization and subsequent death, as other non-ionic detergents/surfactants seem to act, such as Tween and Triton X100 [68,139–142].

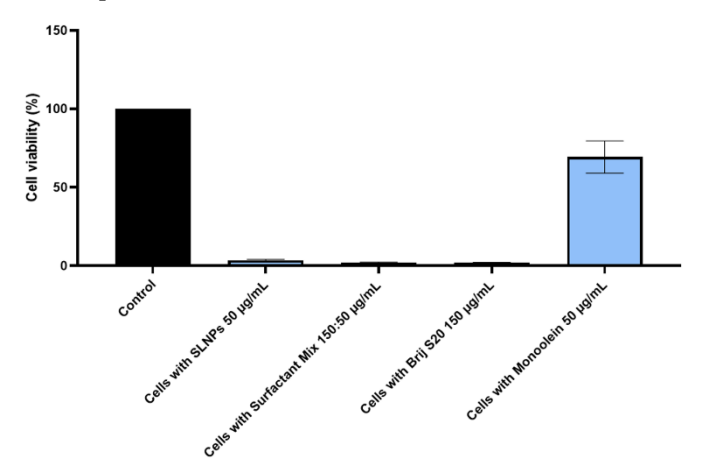


Figure 3.8. Cell viability of hCMEC/D3 cells incubated with 50 μ g/mL of SLNPs and its respective components in the same concentrations.

Values represent the mean \pm SD (n = 5). Cells were incubated with SLNPs (50 μ g/mL), the surfactant mix Brij S20:Monoolein (150:50 μ g/mL), Brij S20 alone (150 μ g/mL) and Monoolein (50 μ g/mL). These results suggest the root of toxicity lies within Brij S20 and not the rest of the SLNPs components.

When SLNPs are produced, as a final step, they can be purified, removing the excess material in solution, as well as the undesirable byproducts of the process. For this, common methods pass through the use of dialysis membranes, removing the unbound surfactant in solution [143,144]. However, the characteristics of this formulation do not allow for these procedures, as micelles can be formed with different sizes, as well as creating structures with the same weight and consequence affinity as the SLNPs are surrounded by the surfactants on their surface. With this, one possible way to purify these samples and remove the excess of surfactant would be through centrifugation. This process could allow for the sedimentation of heavier particles removing the smaller-sized micelles in the supernatant, followed by a second centrifugation step where the heavier and larger unwanted particles would be discarded from solution. However, similar sized SLNPs and micelles would still remain in solution, not fully removing the excess of surfactant in solution.

3.3.3 Optimal surfactant range

With seemingly no possible alternative to work with these stock conditions, this work sought to understand the new ideal concentrations to which the SLNPs could be produced and administered in these studies. It is possible to identify potential optimal working concentrations of both Brij S20, as well as monoolein individually. Since the SLNPs presented to cells have a 1:100 dilution factor, stock solution of both surfactants have 100 times the concentration described, meaning, that the next step of assessing optimal surfactant mix concentration of Brij S20:Monoolein (0.5:5 μ g/mL) required the preparation of a stock solution of 0.5:5 μ g/mL in ultrapure filtered MilliQ water. With this mixture prepared, the cytotoxicity on hCMEC/D3 was assessed. Results are represented in Figure 3.9. It is possible to assume that these optimal concentrations seem not to induce a negative response on the cells, highlighting the promising use of the NPs when considering an appropriate concentration of their surfactants. Not only this, but it is also possible to understand that when mixed, the surfactants can also show a positive effect on cell cytotoxicity as can be seen by the increase in concentrations to 10:100 μ g/mL of Brij S20:Monoolein without a significant toxicity response. This raises the possibility of further increasing the concentrations of Brij S20 as long as the concentration of monoolein also increases within the same proportion without inducing a significant cytotoxic response. This has been considered as a

possibility to solve some toxicity issues of some surfactants, mixing them with other non-toxic ones, hampering this effect, which can be assessed in future work [145].

After identifying the optimal surfactant mixture concentration, a new concern is risen, which is the possibility of producing this same SLNPs with such specific surfactant concentrations. Since the production process of these SLNPs relies on the wetting and nucleus formation processes by the fragmentation of the lipid block, and due to the high hydrophobic nature of ATO 5, similar to other types of SLNPs, the appropriate concentration of surfactants is crucial for the correct production process to be carried out and achieve optimal NP characteristics [70,146]. So, as possible future work, it could be assessed the possibility of these SLNPs to be prepared with these lower surfactant concentrations, as a means to solve the toxicity issues and further improving the system. In a scenario where this concentration does not work, compromising the preparation of the SLNPs, the only possible routes to follow would lead to either remove this surfactant, Brij S20, entirely from solution, either substituting it, or not, by a more biocompatible one, or to improve the purification process to remove this excess.

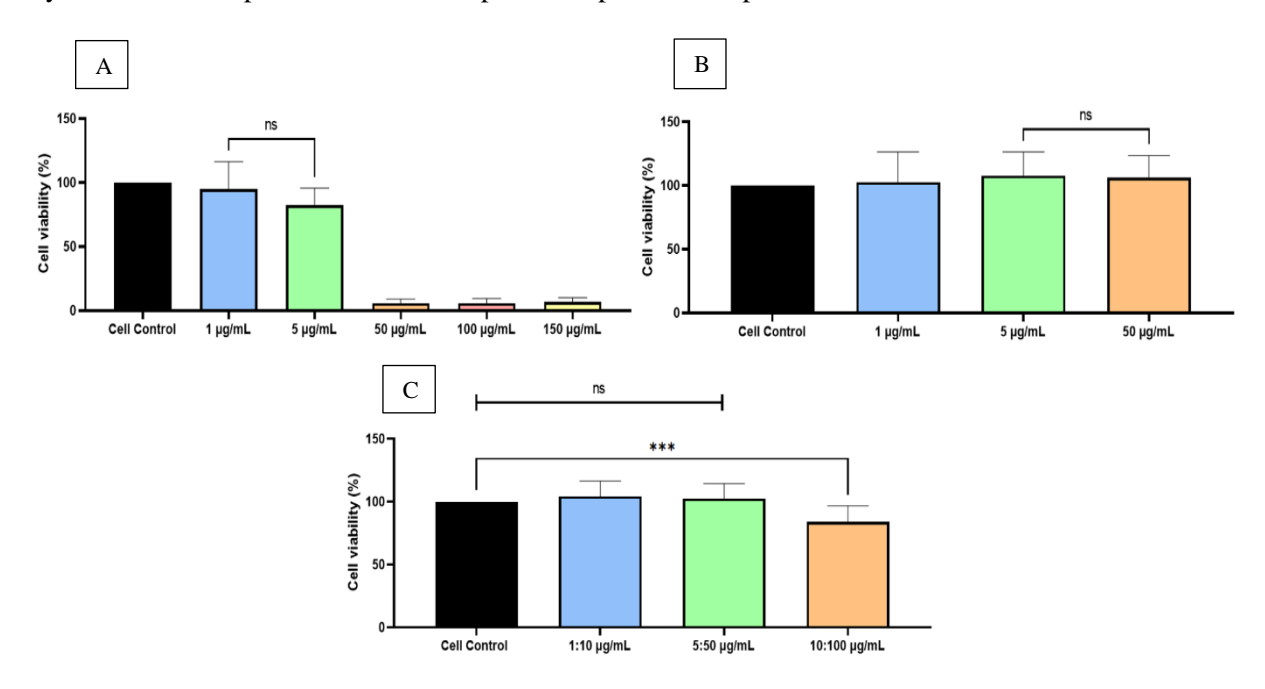


Figure 3.9. Cell viability of hCMEC/D3 cells with different concentrations of individualized surfactants and combined.

(A) hCMEC/D3 cells incubated with 1, 5, 50, 100, 150 μ g/mL of Brij S20 solution and the respective cell control; (B) hCMEC/D3 cells incubated with 1, 5, 50 μ g/mL of Monoolein solution and the respective cell control; (C) Surfactant mix with optimal concentrations of Brij S20:Monoolein 1:10, 5:50, 10:100 μ g/mL. Values represent the mean \pm SD and each condition was tested in three independent assays with five replicates each.

These results prove that, by lowering the Brij S20 concentration in the surfactant mixture, the formulation might not induce cytotoxicity.

3.4 Cell internalization assays

Despite the lack of specificity of the fluorescence signal, as reported in the section **3.1.4 Fluorescent intensity**, the interaction and internalization of SLNPs by hCMEC/D3 cells was still assessed for the concentration of 500 ng/mL. Both Figure 3.10 and Table 3.2 highlight the lack of green (FITC) signal, associated with the SLNPs. Confocal microscopy, allows for the 2D visualization of the cells and the stained components, in this case the nucleus, the filamentous actin and, in the best-case scenario, the SLNPs, understanding where they could be present if they were interacting with the cells. However, as can be seen by the Table 3.2 and Figure 3.10, there is no sign of interaction between the SLNPs and the cells, with them neither being internalized nor adhered to their surface.

Another method to quantify the amount of internalized fluorescent SLNPs by cells is through FACS, which counts the number of events passing through the sensor with the respective wavelength of the probe used. This allows to both quantify the fluorescence signal inside the cells, as well as assess if the SLNPs were internalized or stuck to the surface of the cells or if they did not interact with them at all [81,147]. Since it is possible to understand that these SLNPs interacts with the cells, resulting in their death at the higher concentrations, and once these assays did not produce positive results of interaction, not even showing a green signal, it further enforces the hypothesis that at these concentration there is a lack of SLNPs in solution, with the fluorescent signal visualized in the previous section being only referent to the excess of FITC present in solution rather than associated with the SLNPs. This further highlights the need for the optimization processes related to both the production and post-production treatment of the SLNPs, removing the undesired substances that might be hindering the systems potential.

Table 3.2. hCMEC/D3 SLNPs internalization analyzed by FACS.

Values are presented as mean \pm SD from three independent assays with three replicates each. This technique allows for the quantification of the internalized SLNPs by measuring the fluorescence signal of FITC-labeled SLNPs. These results suggest that there is no uptake of SLNPs by the cells, or there are not enough SLNPs in solution, resulting in the absence of fluorescence measured.

* 100 000 events were counted per replicate, adding to 300 000 events counted for each independent assay.

Sample	Events counted	Signal quantification (%)
Untreated Cells	100 000*	0.015 ± 0.007
Cells treated with SLNPs	100 000*	0.029 ± 0.007

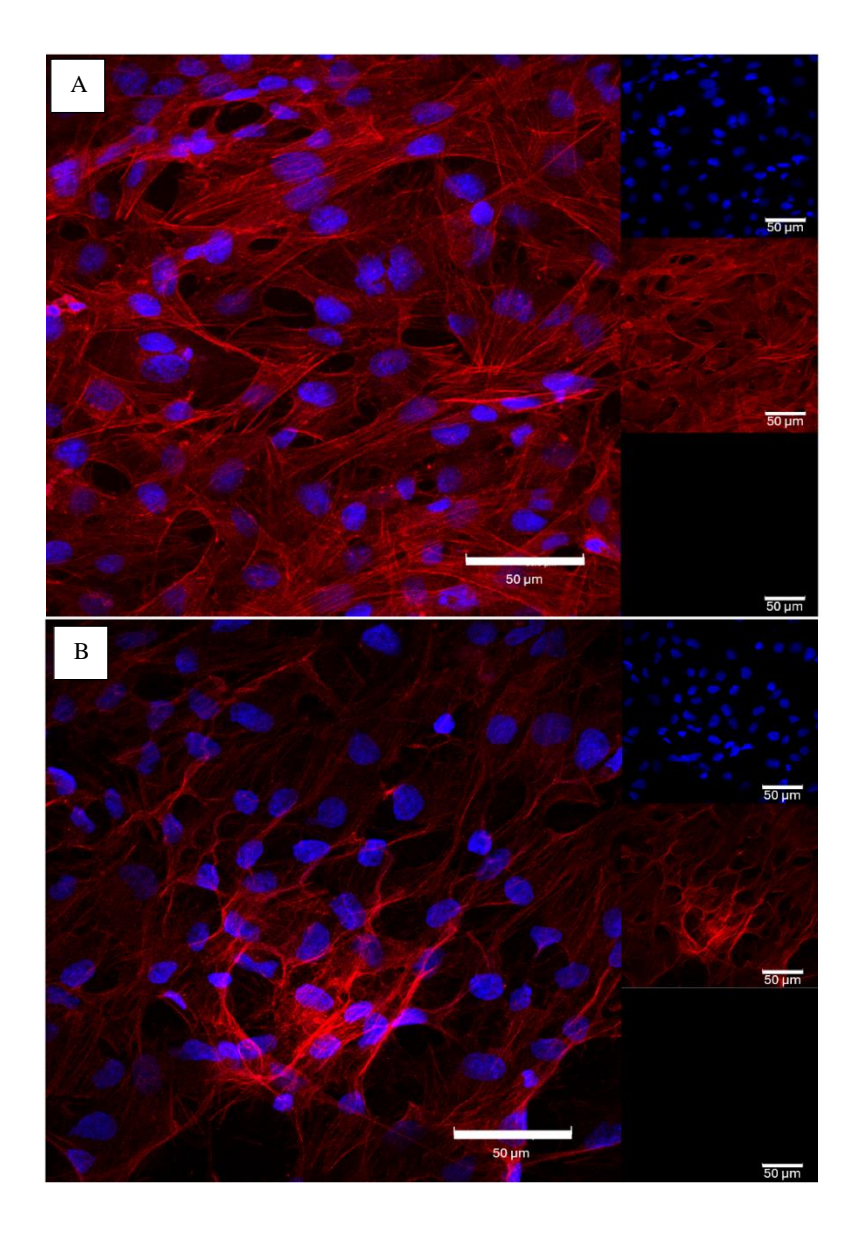


Figure 3.10. Confocal microscopy image of hCMEC/D3 cells untreated with SLNPs (**A**) and after 4h of incubation with 500 ng/mL of SLNPs (**B**).

These images suggest that there are no SLNPs present in the sample, as can be seen by the lack of green signal, further indicating the lack of internalization in the cells.

The images on the right represent the individual colour channels for DAPI, F-Actin and SLNPs (Blue, Red and Green) respectively. (Scale bar: $50 \,\mu m$)

CONCLUSIONS AND FUTURE PERSPEC-TIVES

In the described work, the evaluation of a novel SLNP formulation was assessed, being characterized, and tested in different simulating environments for the assessment of their possible role as drug delivery systems across the BBB in AD environment. These NPs were produced by an unconventional procedure, resulting from the repeated fragmentation of a large lipidic block by thermal-variation cycles, creating smaller nucleated SLNPs composed of Precirol ATO 5 as the lipidic matrix surrounded by Brij S20 and Monoolein as surfactants. These SLNPs had a size of 56.39 ± 0.78 nm and a negative charge (- 9.80 ± 0.81 mV), which presented high stability in different conditions that would simulate cell culture environment and ultimately the physiological conditions of the human body. Stability assessment was however a challenge due to the equipment limitations, highlighting the need for the optimization of characterization protocols. An interesting approach for future work would be to perform kinetic studies of the SLNPs in the different environments, assessing the different properties variations over shorter periods of time. For that, instead of DLS analysis and TEM images, Cryo-Electron Microscopy (CryoEM) would serve as a promising alternative for these assays, as it allows to assess basic sample characteristics, surface interactions and captures dynamic processes over time with high resolution and an accurate representation of the stock solution.

These NPs however, despite promising, fell short on their cellular application, resulting in a decrease in cell viability when presented in concentrations similar to the ones described in the literature. By testing the SLNPs components individually, Brij S20 was found to be the most probable root of the cytotoxic problem, highlighting the need to lower the concentration of this surfactant in the final solution. To achieve this goal, one could either lower the initial concentration of surfactant used in SLNP preparation or try to remove the excess surfactant that might be present in solution and inducing this response. This excess also interferes with the SLNP characterization techniques, resulting in artifacts presented in the different analysis performed throughout this work.

Lowering the SLNP concentration could solve the toxicity problem of this component when incubating the formulation with cells, however, the results presented in this work suggest that at the referred concentrations SLNPs might no longer be present in solution. This would result in the ineffective administration of this system, and subsequent no internalization in human endothelial cells or BBB crossing.

As a final remark, the success of the SLNPs addressed in this work might only be achieved by the implementation of certain changes either in the formulation or on their production process. The excess surfactant removal remains a crucial and focal point for the subsequent studies using these NPs, otherwise their cytotoxic behavior will be persistent. On another hand, this surfactant could also be used in lower concentrations to solve this issue, completely removed from the formulation or, if necessary, exchanged by another that presents a higher degree of biocompatibility and will not induce this response. Alternatively, it would also be interesting to assess different combinations between Brij S20 and Monoolein, changing their proportion, assessing the possibility of the toxic effect being hindered by the presence of monoolein. Only after these changes are performed can one move on to the permeability

studies using *in vitro* BBB models, with its future translation into *in vivo* mice models upon appropriate results. Adding to these assays, it would also be important to assess the ability of these SLNPs to internalize appropriate therapeutic agents for AD, assessing its effectiveness to treat the disease in the appropriate models.

REFERENCES

- [1] L. Thau, V. Reddy, P. Singh, Anatomy, Central Nervous System, in: StatPearls, StatPearls Publishing, Treasure Island (FL), 2022: pp. 478–478. https://www.ncbi.nlm.nih.gov/books/NBK542179/ (accessed July 18, 2024).
- [2] S. Ackerman, Major Structures and Functions of the Brain, in: Discovering the Brain, National Academies Press (US), Washington (DC), 1992. https://www.ncbi.nlm.nih.gov/books/NBK234157/ (accessed July 18, 2024).
- [3] K. Javed, V. Reddy, F. Lui, Neuroanatomy, Cerebral Cortex, in: StatPearls, StatPearls Publishing, Treasure Island (FL), 2023. https://www.ncbi.nlm.nih.gov/books/NBK537247/ (accessed July 18, 2024).
- [4] Z. Arvanitakis, R.C. Shah, D.A. Bennett, Diagnosis and Management of Dementia: A Review, JAMA 322 (2019) 1589–1599.
- [5] X.X. Zhang, Y. Tian, Z.T. Wang, Y.H. Ma, L. Tan, J.T. Yu, The Epidemiology of Alzheimer's Disease Modifiable Risk Factors and Prevention, J Prev Alz Dis 8 (2021) 313–321.
- [6] S. Long, C. Benoist, W. Weidner, World Alzheimer Report 2023 Reducing dementia risk: never too early, never too late, London, 2023. https://www.alzint.org/resource/world-alzheimer-report-2023/ (accessed July 18, 2024).
- [7] Y. Ju, K.Y. Tam, Pathological mechanisms and therapeutic strategies for Alzheimer's disease, Neural Regen Res 17 (2022) 543–549.
- [8] R. Perneczky, F. Jessen, T. Grimmer, J. Levin, A. Flöel, O. Peters, L. Froelich, Anti-amyloid antibody therapies in Alzheimer's disease, Brain 146 (2023) 842–849.
- [9] 2023 Alzheimer's disease facts and figures, Alzheimers Dement 19 (2023) 1598–1695.
- [10] P. Chopade, N. Chopade, Z. Zhao, S. Mitragotri, R. Liao, V. Chandran Suja, Alzheimer's and Parkinson's disease therapies in the clinic, Journal of Bioengineering & Translational Medicine 8 (2023).
- [11] L. Kong, X.T. Li, Y.N. Ni, H.H. Xiao, Y.J. Yao, Y.Y. Wang, R.J. Ju, H.Y. Li, J.J. Liu, M. Fu, Y.T. Wu, J.X. Yang, L. Cheng, Transferrin-modified osthole PEGylated liposomes travel the blood-brain barrier and mitigate alzheimer's disease-related pathology in APP/PS-1 mice, Int J Nanomedicine 15 (2020) 2841–2858.
- [12] M. Callens, N. Kraskovskaya, K. Derevtsova, W. Annaert, G. Bultynck, I. Bezprozvanny, T. Vervliet, The role of Bcl-2 proteins in modulating neuronal Ca2+ signaling in health and in Alzheimer's disease, Biochim Biophys Acta Mol Cell Res 1868 (2021).
- [13] J. Cummings, G. Lee, P. Nahed, M.E.Z.N. Kambar, K. Zhong, J. Fonseca, K. Taghva, Alzheimer's disease drug development pipeline: 2022, Alzheimer's Dement 8 (2022).
- [14] R. Doucette, M. Fisman, V.C. Hachinski, H. Mersky, Cell Loss from the Nucleus Basalis of Meynert in Alzheimer's Disease, Can J Neurol Sci 13 (1986) 435–440.
- [15] Y. Liu, S. An, J. Li, Y. Kuang, X. He, Y. Guo, H. Ma, Y. Zhang, B. Ji, C. Jiang, Brain-targeted co-delivery of therapeutic gene and peptide by multifunctional nanoparticles in Alzheimer's disease mice, Biomaterials 80 (2016) 33–45.

- [16] M.G. Barbato, R.C. Pereira, H. Mollica, A.L. Palange, M. Ferreira, P. Decuzzi, A permeable onchip microvasculature for assessing the transport of macromolecules and polymeric nanoconstructs, J Colloid Interface Sci 594 (2021) 409–423.
- [17] Z. Redzic, Molecular biology of the blood-brain and the blood-cerebrospinal fluid barriers: similarities and differences, Fluids Barriers CNS 8 (2011) 3.
- [18] M.A. Erickson, M.L. Wilson, W.A. Banks, In vitro modeling of blood-brain barrier and interface functions in neuroimmune communication, Fluids Barriers CNS 17 (2020).
- [19] P. Khare, S.X. Edgecomb, C.M. Hamadani, E.E.L. Tanner, D. S Manickam, Lipid nanoparticle-mediated drug delivery to the brain, Adv Drug Deliv Rev 197 (2023).
- [20] R.G.R. Pinheiro, A.J. Coutinho, M. Pinheiro, A.R. Neves, Nanoparticles for targeted brain drug delivery: What do we know?, Int J Mol Sci 22 (2021).
- [21] A.C. Correia, A.R. Monteiro, R. Silva, J.N. Moreira, J.M. Sousa Lobo, A.C. Silva, Lipid nanoparticles strategies to modify pharmacokinetics of central nervous system targeting drugs: Crossing or circumventing the blood–brain barrier (BBB) to manage neurological disorders, Adv Drug Deliv Rev 189 (2022).
- [22] A.E. Alkhalifa, N.F. Al-Ghraiybah, J. Odum, J.G. Shunnarah, N. Austin, A. Kaddoumi, Blood–Brain Barrier Breakdown in Alzheimer's Disease: Mechanisms and Targeted Strategies, Int J Mol Sci 24 (2023).
- [23] A. Reinhold, H. Rittner, Barrier function in the peripheral and central nervous system—a review, Pflugers Arch 469 (2017) 123–134.
- [24] H. Kadry, B. Noorani, L. Cucullo, A blood-brain barrier overview on structure, function, impairment, and biomarkers of integrity, Fluids Barriers CNS 17 (2020).
- [25] E.G. Knox, M.R. Aburto, G. Clarke, J.F. Cryan, C.M. O'Driscoll, The blood-brain barrier in aging and neurodegeneration, Mol Psychiatry 27 (2022) 2659–2673.
- [26] S.R.K. Pandian, K.K. Vijayakumar, S. Murugesan, S. Kunjiappan, Liposomes: An emerging carrier for targeting Alzheimer's and Parkinson's diseases, Heliyon 8 (2022).
- [27] A.M. Grabrucker, B. Ruozi, D. Belletti, F. Pederzoli, F. Forni, M.A. Vandelli, G. Tosi, Nanoparticle transport across the blood brain barrier, Tissue Barriers 4 (2016).
- [28] A. Montagne, Z. Zhao, B. V. Zlokovic, Alzheimer's disease: A matter of blood-brain barrier dysfunction?, World J Exp Med 214 (2017) 3151–3169.
- [29] A. Misra, A. Shahiwala, S.P. Shah, S. Ganesh, Drug delivery to the central nervous system: a review, J Pharm Pharm Sci 6 (2003) 252–273.
- [30] A. Minn, J.F. Ghersi-Egea, R. Perrin, B. Leininger, G. Siest, Drug metabolizing enzymes in the brain and cerebral microvessels, Brain Res Rev 16 (1991) 65–82.
- [31] A.M. Hersh, S. Alomari, B.M. Tyler, Crossing the Blood-Brain Barrier: Advances in Nanoparticle Technology for Drug Delivery in Neuro-Oncology, Int J Mol Sci 23 (2022).
- [32] F. Juhairiyah, E.C.M. de Lange, Understanding Drug Delivery to the Brain Using Liposome-Based Strategies: Studies that Provide Mechanistic Insights Are Essential, AAPS J 23 (2021).
- [33] Y. Shin, S.H. Choi, E. Kim, E. Bylykbashi, J.A. Kim, S. Chung, D.Y. Kim, R.D. Kamm, R.E. Tanzi, Blood–Brain Barrier Dysfunction in a 3D In Vitro Model of Alzheimer's Disease, Adv. Sci. 6 (2019).
- [34] F.L. Cardoso, J. Herz, A. Fernandes, J. Rocha, B. Sepodes, M.A. Brito, D.B. McGavern, D. Brites, Systemic inflammation in early neonatal mice induces transient and lasting neurodegenerative effects, J Neuroinflammation 12 (2015).
- [35] J. Xiang, Y. Tang, C. Li, E.J. Su, D.A. Lawrence, R.F. Keep, Mechanisms Underlying Astrocyte Endfeet Swelling in Stroke, Acta Neurochir Suppl 121 (2016) 19–22. https://pubmed.ncbi.nlm.nih.gov/26463917/ (accessed July 18, 2024).
- [36] P.B.L. Pun, J. Lu, S. Moochhala, Involvement of ROS in BBB dysfunction, Free Radic Res 43 (2009) 348–364.
- [37] S. Liebner, A. Fischmann, G. Rascher, F. Duffner, E.-H. Grote, H. Kallbacher, H. Wolburg, Claudin-1 and claudin-5 expression and tight junction morphology are altered in blood vessels of human glioblastoma multiforme, Acta Neuropathol (2000) 323–331.
- [38] H.E. De Vries, M.C.M. Blom-Roosemalen, M. Van Oosten, A.G. De Boer, T.J.C. Van Berkel, D.D. Breimer, J. Kuiper, The influence of cytokines on the integrity of the blood-brain barrier in vitro, J Neuroimmunol 64 (1996) 37–43.

- [39] J.A. Sousa, C. Bernardes, S. Bernardo-Castro, M. Lino, I. Albino, L. Ferreira, J. Brás, R. Guerreiro, M. Tábuas-Pereira, I. Baldeiras, I. Santana, J. Sargento-Freitas, Reconsidering the role of blood-brain barrier in Alzheimer's disease: From delivery to target, Front Aging Neurosci 15 (2023).
- [40] S.Y. Kook, H.S. Hong, M. Moon, C.M. Ha, S. Chang, I. Mook-Jung, Aβ 1-42-rage interaction disrupts tight junctions of the blood-brain barrier via Ca 2+-calcineurin signaling, J. Neurosci 32 (2012) 8845–8854.
- [41] J. Banerjee, Y. Shi, H.S. Azevedo, In vitro blood–brain barrier models for drug research: state-of-the-art and new perspectives on reconstituting these models on artificial basement membrane platforms, Drug Discov Today 21 (2016) 1367–1386.
- [42] S. Aday, R. Cecchelli, D. Hallier-Vanuxeem, M.P. Dehouck, L. Ferreira, Stem Cell-Based Human Blood-Brain Barrier Models for Drug Discovery and Delivery, Trends Biotechnol 34 (2016) 382–393.
- [43] F. Pfeiffer, J. Schäfer, R. Lyck, V. Makrides, S. Brunner, N. Schaeren-Wiemers, U. Deutsch, B. Engelhardt, Claudin-1 induced sealing of blood-brain barrier tight junctions ameliorates chronic experimental autoimmune encephalomyelitis, Acta Neuropathol 122 (2011) 601–614.
- [44] M.K. Satapathy, T.L. Yen, J.S. Jan, R.D. Tang, J.Y. Wang, R. Taliyan, C.H. Yang, Solid lipid nanoparticles (SLNs): An advanced drug delivery system targeting brain through BBB, Pharmaceutics 13 (2021).
- [45] A.R. Jones, E. V. Shusta, Blood-brain barrier transport of therapeutics via receptor-mediation, Pharm Res 24 (2007) 1759–1771.
- [46] J. Yang, K.M. Luly, J.J. Green, Nonviral nanoparticle gene delivery into the CNS for neurological disorders and brain cancer applications, Wiley Interdiscip Rev Nanomed Nanobiotechnol 15 (2023).
- [47] M. Tsakiri, C. Zivko, C. Demetzos, V. Mahairaki, Lipid-based nanoparticles and RNA as innovative neuro-therapeutics, Front Pharmacol 13 (2022).
- [48] S.M. Lombardo, M. Schneider, A.E. Türeli, N.G. Türeli, Key for crossing the BBB with nanoparticles: The rational design, Beilstein J Nanotechnol 11 (2020) 866–883.
- [49] I. Cacciatore, M. Ciulla, E. Fornasari, L. Marinelli, A. Di Stefano, Solid lipid nanoparticles as a drug delivery system for the treatment of neurodegenerative diseases, Expert Opin Drug Deliv 13 (2016) 1121–1131.
- [50] B. Mekuye, B. Abera, Nanomaterials: An overview of synthesis, classification, characterization, and applications, Nano Select 4 (2023) 486–501.
- [51] S. Malik, J. Singh, R. Goyat, Y. Saharan, V. Chaudhry, A. Umar, A.A. Ibrahim, S. Akbar, S. Ameen, S. Baskoutas, Nanomaterials-based biosensor and their applications: A review, Heliyon 9 (2023).
- [52] Y. Duan, A. Dhar, C. Patel, M. Khimani, S. Neogi, P. Sharma, N. Siva Kumar, R.L. Vekariya, A brief review on solid lipid nanoparticles: Part and parcel of contemporary drug delivery systems, RSC Adv 10 (2020) 26777–26791.
- [53] S. V. Morse, A. Mishra, T.G. Chan, R. T. M. de Rosales, J.J. Choi, Liposome delivery to the brain with rapid short-pulses of focused ultrasound and microbubbles, J Control Release 341 (2022) 605–615.
- [54] M. Yu, J. Zheng, Clearance Pathways and Tumor Targeting of Imaging Nanoparticles, ACS Nano 9 (2015) 6655–6674.
- [55] Y. Liu, J. Hardie, X. Zhang, V.M. Rotello, Effects of engineered nanoparticles on the innate immune system, Semin Immunol 34 (2017) 25–32.
- [56] G. Gul, R. Faller, N. Ileri-Ercan, Polystyrene-modified carbon nanotubes: Promising carriers in targeted drug delivery, Biophys J 121 (2022) 4271–4279.
- [57] R. Mendes, P. Pedrosa, J.C. Lima, A.R. Fernandes, P. V. Baptista, Photothermal enhancement of chemotherapy in breast cancer by visible irradiation of Gold Nanoparticles, Sci Rep 7 (2017) 1–9.
- [58] S.D. Oberdick, K. V. Jordanova, J.T. Lundstrom, G. Parigi, M.E. Poorman, G. Zabow, K.E. Keenan, Iron oxide nanoparticles as positive T1 contrast agents for low-field magnetic resonance imaging at 64 mT, Sci Rep 13 (2023).

- [59] B. Wilson, K.M. Geetha, Lipid nanoparticles in the development of mRNA vaccines for COVID-19, J Drug Deliv Sci Technol 74 (2022).
- [60] M.W. Seo, T.E. Park, Recent advances with liposomes as drug carriers for treatment of neuro-degenerative diseases, Biomed Eng Lett 11 (2021) 211–216.
- [61] L. Li, X. Di, S. Zhang, Q. Kan, H. Liu, T. Lu, Y. Wang, Q. Fu, J. Sun, Z. He, Large amino acid transporter 1 mediated glutamate modified docetaxel-loaded liposomes for glioma targeting, Colloids Surf B Biointerfaces 141 (2016) 260–267.
- [62] J. Chang, Y. Jallouli, M. Kroubi, X. bo Yuan, W. Feng, C. sheng Kang, P. yu Pu, D. Betbeder, Characterization of endocytosis of transferrin-coated PLGA nanoparticles by the blood-brain barrier, Int J Pharm 379 (2009) 285–292.
- [63] S. Li, Z. Peng, J. Dallman, J. Baker, A.M. Othman, P.L. Blackwelder, R.M. Leblanc, Crossing the blood-brain-barrier with transferrin conjugated carbon dots: A zebrafish model study, Colloids Surf B Biointerfaces 145 (2016) 251–256.
- [64] M.G. Shivananjegowda, U. Hani, R.A.M. Osmani, A.H. Alamri, M. Ghazwani, Y. Alhamhoom, M. Rahamathulla, S. Paranthaman, D.V. Gowda, A. Siddiqua, Development and Evaluation of Solid Lipid Nanoparticles for the Clearance of Aβ in Alzheimer's Disease, Pharmaceutics 15 (2023).
- [65] E. Peira, P. Marzola, V. Podio, S. Aime, A. Sbarbati, M.R. Gasco, In Vitro and In Vivo Study of Solid Lipid Nanoparticles Loaded with Superparamagnetic Iron Oxide, J Drug Target 11 (2003) 19–24.
- [66] M.A. Vakilinezhad, A. Amini, H. Akbari Javar, B.F. Baha'addini Beigi Zarandi, H. Montaseri, R. Dinarvand, Nicotinamide loaded functionalized solid lipid nanoparticles improves cognition in Alzheimer's disease animal model by reducing Tau hyperphosphorylation, DARU 26 (2018) 165–177.
- [67] A. Ali, A. Madni, H. Shah, T. Jamshaid, N. Jan, S. Khan, M.M. Khan, M.A. Mahmood, Solid lipid-based nanoparticulate system for sustained release and enhanced in-vitro cytotoxic effect of 5-fluorouracil on skin Melanoma and squamous cell carcinoma, PLoS One 18 (2023).
- [68] S. Obradović, M. Poša, The influence of the structure of selected Brij and Tween homologues on the thermodynamic stability of their binary mixed micelles, J Chem Thermodynamics 110 (2017) 41–50.
- [69] A. Ganem-Quintanar, D. Quintanar-Guerrero, P. Buri, C. Izcalli, Monoolein: A Review of the Pharmaceutical Applications, Drug Dev. Ind. Pharm. 26 (2000) 809–820. www.dekker.com.
- [70] I. Lesov, D. Glushkova, D. Cholakova, M.T. Georgiev, S. Tcholakova, S.K. Smoukov, N. Denkov, Flow reactor for preparation of lipid nanoparticles via temperature variations, J Ind Eng Chem 112 (2022) 37–45.
- [71] C. Gollwitzer, D. Bartczak, H. Goenaga-Infante, V. Kestens, M. Krumrey, C. Minelli, M. Pálmai, Y. Ramaye, G. Roebben, A. Sikora, Z. Varga, A comparison of techniques for size measurement of nanoparticles in cell culture medium, Anal Methods 8 (2016) 5272–5282.
- [72] S. Bhattacharjee, DLS and zeta potential What they are and what they are not?, J Control Release 235 (2016) 337–351.
- [73] G.R. Topal, M. Mészáros, G. Porkoláb, A. Szecskó, T.F. Polgár, L. Siklós, M.A. Deli, S. Veszelka, A. Bozkir, ApoE-targeting increases the transfer of solid lipid nanoparticles with donepezil cargo across a culture model of the blood–brain barrier, Pharmaceutics 13 (2021) 1–19.
- [74] F.H. Santiago-Tirado, R.S. Klein, T.L. Doering, An In Vitro Brain Endothelial Model for Studies of Cryptococcal Transmigration into the Central Nervous System, Curr Protoc Microbiol 53 (2019).
- [75] S. Panico, S. Capolla, S. Bozzer, G. Toffoli, M. Dal Bo, P. Macor, Biological Features of Nanoparticles: Protein Corona Formation and Interaction with the Immune System, Pharmaceutics 14 (2022).
- [76] G. Bashiri, M.S. Padilla, K.L. Swingle, S.J. Shepherd, M.J. Mitchell, K. Wang, Nanoparticle protein corona: from structure and function to therapeutic targeting, Lab Chip 23 (2023) 1432–1466.

- [77] A.R. Neves, J.F. Queiroz, B. Weksler, I.A. Romero, P.O. Couraud, S. Reis, Solid lipid nanoparticles as a vehicle for brain-targeted drug delivery: Two new strategies of functionalization with apolipoprotein E, Nanotechnology 26 (2015).
- [78] A. Trapani, M.Á. Esteban, F. Curci, D.E. Manno, A. Serra, G. Fracchiolla, C. Espinosa-Ruiz, S. Castellani, M. Conese, Solid Lipid Nanoparticles Administering Antioxidant Grape Seed-Derived Polyphenol Compounds: A Potential Application in Aquaculture, Molecules 27 (2022).
- [79] A. Nakhlband, M. Eskandani, N. Saeedi, S. Ghafari, Y. Omidi, J. Barar, A. Garjani, Marrubiin-loaded solid lipid nanoparticles' impact on TNF-α treated umbilical vein endothelial cells: A study for cardioprotective effect, Colloids Surf B Biointerfaces 164 (2018) 299–307.
- [80] A. Casciati, M. Tanori, R. Manczak, S. Saada, B. Tanno, P. Giardullo, E. Porcù, E. Rampazzo, L. Persano, G. Viola, C. Dalmay, F. Lalloué, A. Pothier, C. Merla, M. Mancuso, Human meduloblastoma cell lines: Investigating on cancer stem cell-like phenotype, Cancers (Basel) 12 (2020).
- [81] H.J. Shin, M. Kwak, S. Joo, J.Y. Lee, Quantifying fluorescent nanoparticle uptake in mammalian cells using a plate reader, Sci Rep 12 (2022).
- [82] L. Mihailova, D. Shalabalija, A. Zimmer, N. Geskovski, P. Makreski, M. Petrushevska, M. Simonoska Crcarevska, M. Glavas Dodov, Comparative Studies of the Uptake and Internalization Pathways of Different Lipid Nano-Systems Intended for Brain Delivery, Pharmaceutics 15 (2023).
- [83] J. Dolai, K. Mandal, N.R. Jana, Nanoparticle Size Effects in Biomedical Applications, ACS Appl Nano Mater 4 (2021) 6471–6496. https://pubs.acs.org/doi/full/10.1021/acsanm.1c00987 (accessed August 14, 2024).
- [84] L. Azhar Shekoufeh Bahari, H. Hamishehkar, The Impact of Variables on Particle Size of Solid Lipid Nanoparticles and Nanostructured Lipid Carriers; A Comparative Literature Review., Adv Pharm Bull 6 (2016) 143–51.
- [85] E. Musielak, A. Feliczak-Guzik, I. Nowak, Optimization of the Conditions of Solid Lipid Nanoparticles (SLN) Synthesis, Molecules 27 (2022) 2202.
- [86] P.A. Makoni, K.W. Kasongo, R.B. Walker, Short Term Stability Testing of Efavirenz-Loaded Solid Lipid Nanoparticle (SLN) and Nanostructured Lipid Carrier (NLC) Dispersions, Pharmaceutics 11 (2019) 397.
- [87] D.A. Campos, A.R. Madureira, B. Sarmento, M.M. Pintado, A.M. Gomes, Technological stability of solid lipid nanoparticles loaded with phenolic compounds: Drying process and stability along storage, J Food Eng 196 (2017) 1–10.
- [88] A. del Pozo-Rodríguez, M.A. Solinís, A.R. Gascón, J.L. Pedraz, Short- and long-term stability study of lyophilized solid lipid nanoparticles for gene therapy, Eur J Pharm Biopharm 71 (2009) 181–189.
- [89] A.G. Reinhart, A. Osterwald, P. Ringler, Y. Leiser, M.E. Lauer, R.E. Martin, C. Ullmer, F. Schumacher, C. Korn, M. Keller, Investigations into mRNA Lipid Nanoparticles Shelf-Life Stability under Nonfrozen Conditions, Mol Pharm 20 (2023) 6492–6503.
- [90] M. Koroleva, I. Portnaya, E. Mischenko, I. Abutbul-Ionita, L. Kolik-Shmuel, D. Danino, Solid lipid nanoparticles and nanoemulsions with solid shell: Physical and thermal stability, J Colloid Interface Sci 610 (2022) 61–69.
- [91] M. Danaei, M. Dehghankhold, S. Ataei, F. Hasanzadeh Davarani, R. Javanmard, A. Dokhani, S. Khorasani, M.R. Mozafari, Impact of Particle Size and Polydispersity Index on the Clinical Applications of Lipidic Nanocarrier Systems, Pharmaceutics 10 (2018) 57.
- [92] L. Gastaldi, L. Battaglia, E. Peira, D. Chirio, E. Muntoni, I. Solazzi, M. Gallarate, F. Dosio, Solid lipid nanoparticles as vehicles of drugs to the brain: Current state of the art, Eur J Pharm Biopharm 87 (2014) 433–444.
- [93] M.I. Teixeira, C.M. Lopes, M.H. Amaral, P.C. Costa, Surface-modified lipid nanocarriers for crossing the blood-brain barrier (BBB): A current overview of active targeting in brain diseases, Colloids Surf B Biointerfaces 221 (2023) 112999.
- [94] D. Chirio, M. Gallarate, E. Peira, L. Battaglia, E. Muntoni, C. Riganti, E. Biasibetti, M.T. Capucchio, A. Valazza, P. Panciani, M. Lanotte, L. Annovazzi, V. Caldera, M. Mellai, G. Filice, S. Corona, D. Schiffer, Positive-charged solid lipid nanoparticles as paclitaxel drug delivery system in glioblastoma treatment, Eur J Pharm Biopharm 88 (2014) 746–758.

- [95] A.L. Onugwu, C.S. Nwagwu, O.S. Onugwu, A.C. Echezona, C.P. Agbo, S.A. Ihim, P. Emeh, P.O. Nnamani, A.A. Attama, V. V. Khutoryanskiy, Nanotechnology based drug delivery systems for the treatment of anterior segment eye diseases, Journal of Controlled Release 354 (2023) 465–488.
- [96] A. Nazarova, L. Yakimova, D. Filimonova, I. Stoikov, Surfactant Effect on the Physicochemical Characteristics of Solid Lipid Nanoparticles Based on Pillar[5]arenes, Int J Mol Sci 23 (2022).
- [97] J. Feng, Z. Valkova, E.E. Lin, E. Nourafkan, T. Wang, S. Tcholakova, R. Slavchov, S.K. Smoukov, Minimum surfactant concentration required for inducing self-shaping of oil droplets and competitive adsorption effects, Soft Matter 18 (2022) 6729–6738.
- [98] R. Toy, P.M. Peiris, K.B. Ghaghada, E. Karathanasis, Shaping Cancer Nanomedicine: The Effect of Particle Shape on The In Vivo Journey of Nanoparticles, Nanomedicine 9 (2014) 121–134.
- [99] A.M. El Badawy, T.P. Luxton, R.G. Silva, K.G. Scheckel, M.T. Suidan, T.M. Tolaymat, Impact of environmental conditions (pH, ionic strength, and electrolyte type) on the surface charge and aggregation of silver nanoparticles suspensions, Environ Sci Technol 44 (2010) 1260–1266.
- [100] I. Fernando, Y. Zhou, Impact of pH on the stability, dissolution and aggregation kinetics of silver nanoparticles, Chemosphere 216 (2019) 297–305.
- [101] A.M.N. Silva, X. Kong, R.C. Hider, Determination of the pKa value of the hydroxyl group in the α-hydroxycarboxylates citrate, malate and lactate by 13C NMR: Implications for metal coordination in biological systems, BioMetals 22 (2009) 771–778.
- [102] Y. Zeng, X. Chen, D. Zhao, H. Li, Y. Zhang, X. Xiao, Estimation of pKa values for carboxylic acids, alcohols, phenols and amines using changes in the relative Gibbs free energy, Fluid Phase Equilib 313 (2012) 148–155. https://doi.org/10.1016/j.fluid.2011.09.022.
- [103] J.R. Loften, J.G. Linn, J.K. Drackley, T.C. Jenkins, C.G. Soderholm, A.F. Kertz, Invited review: Palmitic and stearic acid metabolism in lactating dairy cows, J Dairy Sci 97 (2014) 4661–4674.
- [104] A.R. Jose, U. Sivasankaran, S. Menon, K.G. Kumar, A silicon nanoparticle based turn off fluorescent sensor for sudan I, Anal Methods 8 (2016) 5701–5706.
- [105] A.T. Mohi, H.A.A.A. Alreda, Solvent Effect on the spectral and photophysical properties of the Acridone, J Phys Conf Ser 2322 (2022).
- [106] X. Qin, X. Yang, L. Du, M. Li, Polarity-based fluorescence probes: properties and applications, RSC Med Chem 12 (2021) 1826–1838.
- [107] M.A. Haidekker, T.P. Brady, D. Lichlyter, E.A. Theodorakis, Effects of solvent polarity and solvent viscosity on the fluorescent properties of molecular rotors and related probes, Bioorg Chem 33 (2005) 415–425.
- [108] J.R. Lakowicz, Effects of Solvents on Fluorescence Emission Spectra, in: Principles of Fluorescence Spectroscopy, Springer, Boston, MA, 1983: pp. 187–215. https://doi.org/10.1007/978-1-4615-7658-7_7 (accessed August 18, 2024).
- [109] E.A. Slyusareva, M.A. Gerasimov, A.G. Sizykh, L.M. Gornostaev, OPTICS AND SPECTROS-COPY SPECTRAL AND FLUORESCENT INDICATION OF THE ACID-BASE PROPERTIES OF BIOPOLYMER SOLUTIONS, Russian Physics Journal 54 (2011).
- [110] B. Gauthier-Manuel, C. Benmouhoub, B. Wacogne, Fluorescence Spectra of Prototropic Forms of Fluorescein and Some Derivatives and Their Potential Use for Calibration-Free pH Sensing, Sensors 24 (2024).
- [111] T.C. Brelje, M.W. Wessendorf, R.L. Sorenson, Multicolor Laser Scanning Confocal Immunofluorescence Microscopy: Practical Application and Limitations, Methods Cell Biol 70 (2002) 165–249e.
- [112] M. Salari, D. Bitounis, K. Bhattacharya, G. Pyrgiotakis, Z. Zhang, E. Purington, W. Gramlich, Y. Grondin, R. Rogers, D. Bousfield, P. Demokritou, Development & characterization of fluorescently tagged nanocellulose for nanotoxicological studies, Environ Sci Nano 6 (2019) 1516–1526
- [113] C. Freitas, R.H. Mü, Effect of light and temperature on zeta potential and physical stability in solid lipid nanoparticle (SLNTM) dispersions, Int J Pharm 168 (1998) 221–229.
- [114] A. Dutta, A. Paul, A. Chattopadhyay, The effect of temperature on the aggregation kinetics of partially bare gold nanoparticles, RSC Adv 6 (2016) 82138–82149.

- [115] L. Wang, X. Yang, Q. Wang, Y. Zeng, L. Ding, W. Jiang, Effects of ionic strength and temperature on the aggregation and deposition of multi-walled carbon nanotubes, J Environ Sci (China) 51 (2017) 248–255.
- [116] M.D. Leach, L.E. Cowen, Membrane fluidity and temperature sensing are coupled via circuitry comprised of Ole1, Rsp5, and Hsf1 in Candida albicans, Eukaryot Cell 13 (2014) 1077–1084.
- [117] B. Michen, C. Geers, D. Vanhecke, C. Endes, B. Rothen-Rutishauser, S. Balog, A. Petri-Fink, Avoiding drying-artifacts in transmission electron microscopy: Characterizing the size and colloidal state of nanoparticles, Sci Rep 5 (2015).
- [118] N. Wangoo, J. Kaushal, K.K. Bhasin, S.K. Mehta, C.R. Suri, Zeta potential based colorimetric immunoassay for the direct detection of diabetic marker HbA1c using gold nanoprobes, Chemical Communications 46 (2010) 5755–5757.
- [119] V. Selvamani, Stability Studies on Nanomaterials Used in Drugs, in: Characterization and Biology of Nanomaterials for Drug Delivery: Nanoscience and Nanotechnology in Drug Delivery, Elsevier, 2019: pp. 425–444. https://doi.org/10.1016/B978-0-12-814031-4.00015-5 (accessed August 18, 2024).
- [120] M.J. Mitchell, O.E. Jensen, K.A. Cliffe, M.M. Maroto-Valer, A model of carbon dioxide dissolution and mineral carbonation kinetics, Proc R Soc A 466 (2010) 1265–1290.
- [121] M. Mahmoudi, M.P. Landry, A. Moore, R. Coreas, The protein corona from nanomedicine to environmental science, Nat Rev Mater 8 (2023) 422–438. https://doi.org/10.1038/s41578-023-00552-2.
- [122] W. WU, Q. WU, Q. LIU, Y. LI, P. REN, Y. WU, F. CHEN, Identification and characterization of soft protein corona absorbed on iron oxide nanoparticles, Chinese Journal of Analytical Chemistry 51 (2023). https://doi.org/10.1016/j.cjac.2023.100246.
- [123] M. Kokkinopoulou, J. Simon, K. Landfester, V. Mailänder, I. Lieberwirth, Visualization of the protein corona: Towards a biomolecular understanding of nanoparticle-cell-interactions, Nanoscale 9 (2017) 8858–8870.
- [124] L.E. González-García, M.N. Macgregor, R.M. Visalakshan, A. Lazarian, A.A. Cavallaro, S. Morsbach, A. Mierczynska-Vasilev, V. Mailänder, K. Landfester, K. Vasilev, Nanoparticles Surface Chemistry Influence on Protein Corona Composition and Inflammatory Responses, Nanomaterials 12 (2022).
- [125] K. Partikel, R. Korte, N.C. Stein, D. Mulac, F.C. Herrmann, H.U. Humpf, K. Langer, Effect of nanoparticle size and PEGylation on the protein corona of PLGA nanoparticles, Eur J Pharm Biopharm 141 (2019) 70–80.
- [126] D. Čirin, V. Krstonošić, D. Sazdanić, Synergism and antagonism in mixed monolayers: Brij S20/poloxamer 407 and Triton X-100/poloxamer 407 mixtures, Fluid Phase Equilib 473 (2018) 220–225.
- [127] X. Bai, J. Wang, Q. Mu, G. Su, In vivo Protein Corona Formation: Characterizations, Effects on Engineered Nanoparticles' Biobehaviors, and Applications, Front Bioeng Biotechnol 9 (2021).
- [128] F.S.M. Tekie, M. Hajiramezanali, P. Geramifar, M. Raoufi, R. Dinarvand, M. Soleimani, F. Atyabi, Controlling evolution of protein corona: a prosperous approach to improve chitosan-based nanoparticle biodistribution and half-life, Sci Rep 10 (2020) 9664.
- [129] M. Barz, W.J. Parak, R. Zentel, Concepts and Approaches to Reduce or Avoid Protein Corona Formation on Nanoparticles: Challenges and Opportunities, Advanced Science (2024) 2402935.
- [130] H.J. Rodríguez-Franco, J. Weiden, M.M.C. Bastings, Stabilizing Polymer Coatings Alter the Protein Corona of DNA Origami and Can Be Engineered to Bias the Cellular Uptake, ACS Polymers Au 3 (2023) 344–353.
- [131] I. Wong, C.M. Ho, Surface molecular property modifications for poly(dimethylsiloxane) (PDMS) based microfluidic devices, Microfluid Nanofluidics 7 (2009) 291–306.
- [132] D.A. Narváez-Narváez, M. Duarte-Ruiz, S. Jiménez-Lozano, C. Moreno-Castro, R. Vargas, A. Nardi-Ricart, E. García-Montoya, P. Pérez-Lozano, J.M. Suñé-Negre, C. Hernández-Munain, C. Suñé, M. Suñé-Pou, Comparative Analysis of the Physicochemical and Biological Characteristics of Freeze-Dried PEGylated Cationic Solid Lipid Nanoparticles, Pharmaceuticals 16 (2023).
- [133] S. Faes, E. Uldry, A. Planche, T. Santoro, C. Pythoud, N. Demartines, O. Dormond, Acidic pH reduces VEGF-mediated endothelial cell responses by downregulation of VEGFR-2; relevance for anti-angiogenic therapies, Oncotarget 7 (2016) 86026–86038.

- [134] T.L. Riss, R.A. Moravec, A.L. Niles, S. Duellman, H.A. Benink, T.J. Worzella, L. Minor, Cell Viability Assays, in: Assay Guidance Manual, 2013. https://www.ncbi.nlm.nih.gov/books/NBK144065/ (accessed August 19, 2024).
- [135] N. Kumar, R. Afjei, T.F. Massoud, R. Paulmurugan, Comparison of cell-based assays to quantify treatment effects of anticancer drugs identifies a new application for Bodipy-L-cystine to measure apoptosis, Sci Rep 8 (2018).
- [136] R. DEVI, S. AGARWAL, SOME MULTIFUNCTIONAL LIPID EXCIPIENTS AND THEIR PHARMACEUTICAL APPLICATIONS, Int J Pharm Pharm Sci 11 (2019) 1–7.
- [137] M.F. Zaccaro Scelza, L.R. Lima Oliveira, F.B. Carvalho, S. Côrte-Real Faria, In vitro evaluation of macrophage viability after incubation in orange oil, eucalyptol, and chloroform, Oral Surg Oral Med Oral Pathol Oral Radiol Endod. 102 (2006) e24–e27.
- [138] P. Mura, F. Maestrelli, M. D'Ambrosio, C. Luceri, M. Cirri, Evaluation and comparison of solid lipid nanoparticles (SLNs) and nanostructured lipid carriers (NLCs) as vectors to develop hydrochlorothiazide effective and safe pediatric oral liquid formulations, Pharmaceutics 13 (2021).
- [139] Z. Amidzadeh, A. Behzad Behbahani, N. Erfani, S. Sharifzadeh, R. Ranjbaran, L. Moezi, F. Aboualizadeh, M.A. Okhovat, P. Alavi, N. Azarpira, Assessment of Different Permeabilization Methods of Minimizing Damage to the Adherent Cells for Detection of Intracellular RNA by Flow Cytometry, Avicenna J Med Biotechnol 6 (2013) 38–46.
- [140] B. Arechabala, C. Coiffard, P. Rivalland, L.J.M. Coiffard, Y. De Roeck-Holtzhauer, Comparison of cytotoxicity of various surfactants tested on normal human fibroblast cultures using the neutral red test, MTT assay and LDH release, J Appl Toxicol 19 (1999) 163–165.
- [141] Z. Liu, R. Bendayan, X.Y. Wu, Triton-X-100-modified polymer and microspheres for reversal of multidrug resistance, J Pharm Pharmacol 53 (2010) 779–787.
- [142] M. Poša, A. Pilipović, Activity Coefficient of Triton X100 and Brij S20 in the Infinitely Diluted Micellar Pseudophase of the Binary Micelle Triton X100-Brij S20 in the Water Phase at the Temperature Interval T = (283.15-318.15) K, J Chem Eng Data 65 (2020) 106–119.
- [143] J. Milsmann, K. Oehlke, K. Schrader, R. Greiner, A. Steffen-Heins, Fate of edible solid lipid nanoparticles (SLN) in surfactant stabilized o/w emulsions. Part 1: Interplay of SLN and oil droplets, Colloids Surf A Physicochem Eng Asp 558 (2018) 615–622.
- [144] G.I. Sakellari, I. Zafeiri, H. Batchelor, F. Spyropoulos, Solid lipid nanoparticles and nanostructured lipid carriers of dual functionality at emulsion interfaces. Part I: Pickering stabilisation functionality, Colloids Surf A Physicochem Eng Asp 654 (2022).
- [145] L.Y. Zakharova, T.N. Pashirova, S. Doktorovova, A.R. Fernandes, E. Sanchez-Lopez, A.M. Silva, S.B. Souto, E.B. Souto, Cationic surfactants: Self-assembly, structure-activity correlation and their biological applications, Int J Mol Sci 20 (2019).
- [146] W. Mehnert, K. Mäder, Solid lipid nanoparticles: Production, characterization and applications, Adv Drug Deliv Rev 64 (2012) 83–101.
- [147] A. Rigo, F. Vinante, Flow cytometry analysis of receptor internalization/shedding, Cytometry B Clin Cytom 92 (2017) 291–298.

APPENDIX

A.1 DLS results of the surfactant samples

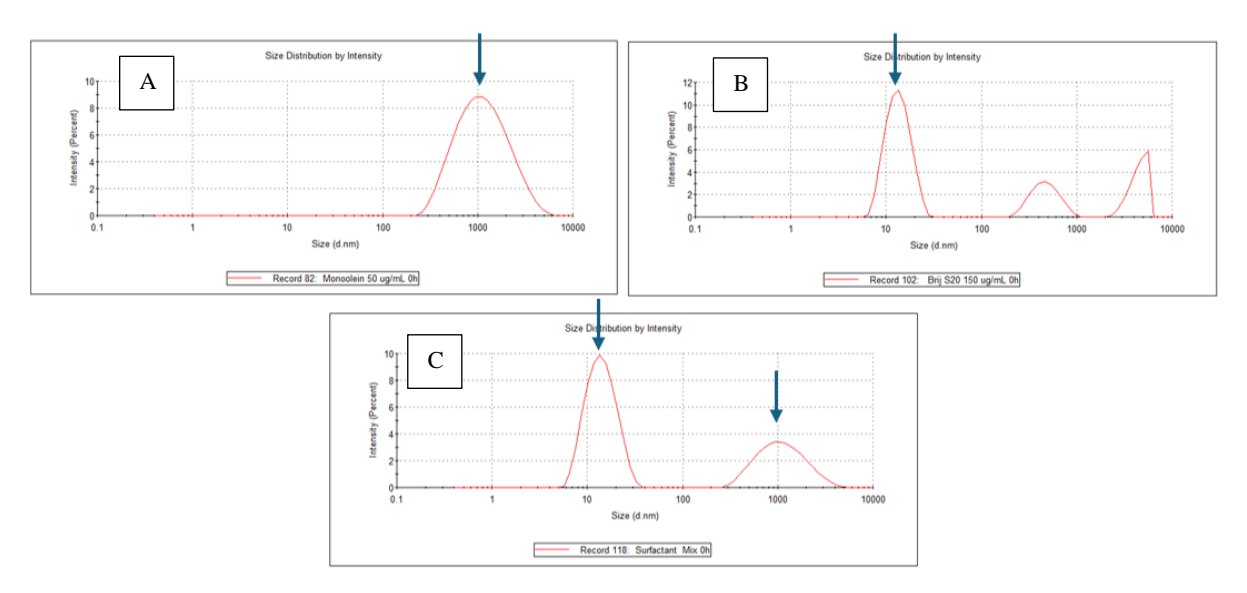


Figure A.1. Raw DLS results of surfactant samples with their representative peaks highlighted by the arrows.

(**A**) Monoolein (50 μg/mL); (**B**) Brij S20 (150 μg/mL); (**C**) Brij S20:Monoolein (150:50 μg/mL).

A.2 DLS results of SLNPs incubated at 37 °C over time

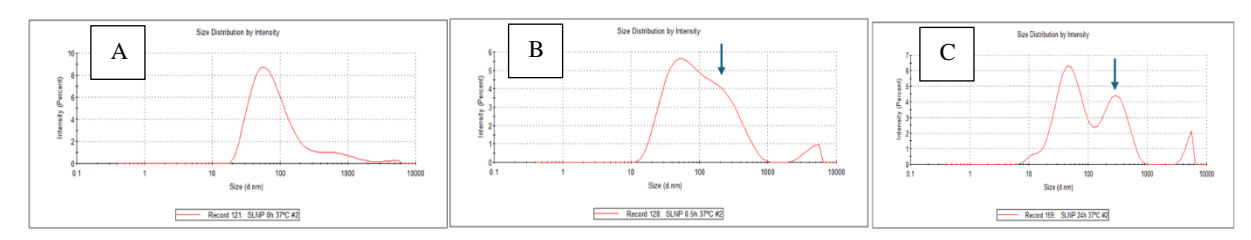


Figure A.2. Raw DLS results of SLNPs incubated in water at 37 °C over different time periods. The arrows depict the appearance of a second peak associated with SLNP cluster formation without aggregation. **(A)** 0h of incubation; **(B)** 30 min of incubation; **(C)** 24h of incubation.



ALEXANDRE GIL